

1 **The Holocene sedimentary record of cyanobacterial
2 glycolipids in the Baltic Sea: Evaluation of their application as
3 tracers of past nitrogen fixation**

4 Martina Sollai¹, Ellen C. Hopmans¹, Nicole J. Bale¹, Anchelique Mets¹, Lisa Warden¹,
5 Matthias Moros² and Jaap S. Sinninghe Damst  ^{1,3}

6
7 ¹NIOZ Royal Netherlands Institute for Sea Research, Department of Marine Microbiology
8 and Biogeochemistry, and Utrecht University, P.O. Box 59, 179AB Den Burg, Texel, The
9 Netherlands.

10 ²Leibniz Institute for Baltic Sea Research (IOW), Department of Marine Geology,
11 Warnem  nde, Germany.

12 ³University of Utrecht, Faculty of Geosciences, Department of Earth Sciences, P.O. Box
13 80.021, 3508 TA Utrecht, The Netherlands.

14
15 Correspondence to: Jaap Sinninghe Damst   (jaap.damste@nioz.nl)

17 **Abstract.** Heterocyst glycolipids (HGs) are lipids exclusively produced by heterocystous
18 dinitrogen-fixing cyanobacteria. The Baltic Sea is an ideal environment to study the
19 distribution of HGs and test their potential as biomarkers because of its recurring summer
20 phytoplankton blooms, dominated by a few heterocystous cyanobacterial species of the
21 genera *Nodularia* and *Aphanizomenon*. A multicore and a gravity core from the Gotland basin
22 were analyzed to determine the abundance and distribution of a suite of selected HGs at high
23 resolution to investigate the changes in past cyanobacterial communities during the Holocene.
24 The HG distribution of the sediments deposited during the Modern Warm Period (MoWP)
25 was compared with those of cultivated heterocystous cyanobacteria, including those isolated
26 from Baltic Sea waters, revealing high similarity. However, the abundance of HGs dropped
27 substantially with depth and this may be caused by either a decrease in the occurrence of the
28 cyanobacterial blooms or diagenesis, resulting in partial destruction of the HGs. The record
29 also shows that the HG distribution has remained stable since the Baltic turned into a brackish
30 semi-enclosed basin ~7200 Cal. yrs BP. This suggests that the heterocystous cyanobacterial
31 species composition remained relatively stable as well. During the earlier freshwater phase of
32 the Baltic (i.e. the Ancylus Lake and Yoldia Sea phases) the distribution of the HGs varied
33 much more than in the subsequent brackish phase and the absolute abundance of HGs was
34 much lower than during the brackish phase. This suggests that the cyanobacterial community
35 adjusted to the different environmental conditions in the basin. Our results confirm the

1 potential of HGs as specific biomarker of heterocystous cyanobacteria in paleo-environmental
2 studies.

3 **1 Introduction**

4 Cyanobacteria are a broad and diverse group of photoautotrophic bacteria; they are found in
5 many terrestrial and aquatic environments (Whitton and Potts, 2012). They can exist as
6 benthos or plankton, unicellular or filamentous with or without branches, free-living or
7 endosymbionts (Rippka et al., 1979) and are of biogeochemical significance due to their role
8 in the cycling of carbon and nitrogen through photosynthesis and the fixation of N₂. However,
9 some N₂-fixing cyanobacteria can negatively impact aquatic ecosystems due to their role in
10 harmful algal blooms (HABs): exceptional events of phytoplankton growth causing
11 anomalous feedbacks on food webs, alteration in the geochemical features of the water
12 column (e.g. anoxia), and sometimes the release of harmful toxins in the environment.
13 Cyanobacterial HABs (cHABs) affect the surface of lacustrine, estuarine and tropical marine
14 environments worldwide; human-induced global warming and nutrient overload are blamed
15 for exacerbating the phenomenon (Paerl, 1988; Paerl et al., 2011; Paerl and Huisman, 2009).

16 The two processes of photosynthesis and N₂ fixation are theoretically incompatible
17 since the nitrogenase enzyme that catalyzes nitrogen fixation is inactivated by O₂. To cope
18 with this, N₂-fixing cyanobacteria have developed several strategies (Stal, 2009). The
19 filamentous diazotrophs of the orders *Nostocales* and *Stigonematales* spatially separate the
20 two metabolisms by forming special cells dedicated to the fixation of N₂, called heterocysts
21 (Wolk, 1982; Adams, 2000). Gas exchange is believed to be regulated by the heterocyst cell
22 wall, which consists of two separate polysaccharide and glycolipid layers (Murry and Wolk,
23 1989; Walsby, 1985) of which the latter acts as the gas diffusion barrier. These so called
24 heterocyst glycolipids (HG)s have been found to date to be unique to heterocyst-forming
25 cyanobacteria (Bryce et al., 1972; Nichols and Wood, 1968) and furthermore their
26 composition has been discovered to be distinct at the level of families and even genera
27 (Bauersachs et al., 2009a, 2014a; Gambacorta et al., 1998; Schouten et al., 2013). Their
28 structure comprises a sugar moiety glycosidically bound to a long *n*-alkyl chain (Fig. 1) with
29 an even number of carbon atoms (26 to 32) with various functional groups (hydroxyl and keto
30 groups) located at the C-3, ω -1 and ω -3 positions (Gambacorta et al., 1995, 1998; Schouten et
31 al., 2013). The sugar moiety of HGs found in non-symbiotic cyanobacteria is typically a
32 hexose (hereafter C₆) (Bryce et al., 1972; Lambein and Wolk, 1973; Nichols and Wood,

1 1968), while HGs associated with endosymbiotic heterocystous cyanobacteria have a pentose
2 moiety (hereafter C₅) (Bale et al., 2015, 2017; Schouten et al., 2013). High-performance
3 liquid chromatography coupled to electrospray ionization tandem mass spectrometry
4 (HPLC/ESI-MS²) has emerged as a rapid method to analyze HGs in cultures (Bauersachs et
5 al., 2009c, 2009a, 2014a) and modern day ecosystems such as microbial mats, lakes and
6 marine systems (Bale et al., 2015, 2016, 2017; Bauersachs et al., 2009c, 2011, 2013, 2015;
7 Wörmer et al., 2012).

8 C₆ HGs have been applied as specific paleo-biomarkers for the presence of N₂-fixing
9 cyanobacteria in marine geological records back to the Pleistocene, and lacustrine deposits
10 back to the Eocene and hence have provided evidence of the high potential for HGs
11 preservation in sedimentary records (Bauersachs et al., 2010). In addition, temperature-
12 induced modifications of the HG composition of heterocystous cyanobacteria were observed
13 both in culture and in the environment and quantified by specific indices, suggesting the
14 possible employment of HGs in reconstructing surface water temperatures (SWT)
15 (Bauersachs et al., 2009a, 2014b, 2015). However, in general, the application of HGs as
16 biomarker in environmental and paleo-environmental studies is still limited.

17 The Baltic Sea, characterized by the seasonal occurrence of cHABs mainly consisting
18 of the HG-producing family *Nostocaceae*, presents an interesting location to both apply HGs
19 as biomarkers in the present day system and to investigate their potential as proxies for
20 reconstruction of past depositional environments. The modern Baltic, one of world's largest
21 brackish bodies of water, is a shallow, semi-enclosed basin, characterized by estuarine
22 circulation, having its only connection to the North Sea through the Danish straits (Fig. 2).
23 Irregular winter inflows of marine oxygen-rich water, known as salinity pulses, represent the
24 main mechanism of renewing and mixing of the bottom water, which otherwise experiences
25 stagnation and increasing oxygen depletion with permanent stratification and persisting
26 anoxia in its deep waters (Kononen et al., 1996). Since the last deglaciation (ca. 13-9 cal. kyr
27 BP) the Baltic Sea has experienced specific hydrographical phases (Andrén et al., 2011).
28 Following the ice retreat, the Baltic Ice Lake developed, which was followed by the Yoldia
29 Sea phase, a short period when there was a connection with the sea. The subsequent Ancylus
30 Lake phase (ca. 9.5–8.0 cal. kyr BP) was the last extended freshwater phase in the basin
31 before a stable connection to the North Sea was established (Björck, 1995; Jensen et al.,
32 1999). The transition phase began (ca. 7.8–7.3 cal. kyr BP) by a series of weak inflows of
33 saline water, which eventually lead to the fully brackish Littorina Sea phase (~7.2–3.5 cal. kyr
34 BP). The less brackish post-Littorina Sea phase (until ~1.3 cal. kyr BP) followed, and the

1 modern Baltic Sea is considered its natural continuation. In the last 1000 yr three alternating
2 periods occurred: the Medieval Warm Period (MWP), the Little Ice Age (LIA) and the current
3 Modern Warm Period (MoWP, starting at ~1950) (Kabel et al., 2012).

4 The modern Baltic undergoes summer cHABs primarily composed of a few species of
5 filamentous heterocystous cyanobacteria *Nodularia spumigena*, *Aphanizomenon flos-aquae*
6 and *Anabaena* spp. (Celepli et al., 2017; Hajdu et al., 2007; Hälfors, 2004; Kanoshina et al.,
7 2003; Karjalainen et al., 2007; Ploug, 2008; Sivonen et al., 2007). Deep water anoxia, high
8 phosphorus availability, calm water conditions and high irradiation resulting in relatively high
9 sea surface temperature (SST) have been identified as main triggers for these blooms. Anoxic
10 sediments lead to the release of phosphate in the water column, stimulating new cHABs and
11 further enhancing anoxia, resulting in a reinforcing feedback (Finni et al., 2001; Kabel et al.,
12 2012; Paerl, 2008; Paerl et al., 2011; Poutanen and Nikkilä, 2001; Stipa, 2002). The summer
13 cHABs have been documented since the 19th century, with a reported increase in their
14 frequency and intensity in the last 60 years, which has been related to human-induced
15 eutrophication (Bianchi et al., 2000; Finni et al., 2001).

16 Several studies, based on fossil pigment and other paleo proxy records, suggest that
17 cHABs have been recurring through the entire Holocene simultaneously with anoxic events
18 and thus should be considered a natural feature of the basin, rather than a consequence of
19 human impact (Bianchi et al., 2000; Borgendahl and Westman, 2007; Funkey et al., 2014;
20 Poutanen and Nikkilä, 2001). SST has been suggested to have played an important role in
21 these events (Kabel et al., 2012; Warden, 2017). Likely, at times of water column
22 stratification and anoxia, high SST would have initiated cHABs in the basin, when exceeding
23 a threshold temperature of ~16 °C, which is considered a trigger to the onset of the cHABs in
24 the modern Baltic (Kononen, 1992; Wasmund, 1997). In addition, this would have enhanced
25 the oxygen consumption of the deep water (Kabel et al., 2012).

26 The intrinsic occurrence of cHABs and their role in intensifying chronic anoxic events
27 is not limited to the Baltic Sea. These same features have been observed in various stratified
28 fresh water lakes in the Northern hemisphere (Fritz, 1989; McGowan et al., 1999; Schweger
29 and Hickman, 1989; Züllig, 1986). However, there is no full agreement on this interpretation,
30 as other authors argue that human perturbation has to be considered to be the main driving
31 force behind the co-occurrence of cHABs with anoxia in the Baltic (Zillén and Conley, 2010).
32 Therefore, more research is required to elucidate the relationship between recurring anoxic
33 events and cHABs in the Baltic Sea.

1 In this study, we test the potential of HGs as paleo-proxy to investigate the changes in
2 past communities involved in the summer cHABs in the Baltic Sea over the Holocene and the
3 potential relationship with the anoxic events that occurred in the basin. To this end, a
4 multicore and a gravity core from the Gotland basin were analyzed for HGs at high resolution.
5 The results of the analysis were compared with the total organic carbon content and the
6 nitrogen isotope record. This may help in further confirming the potential of HGs as specific
7 biomarkers of heterocystous cyanobacteria in environmental studies.

8 **2 Materials and methods**

9 **2.1 Sample site and sediment cores**

10 Our sampling site is located in the Eastern Gotland Basin, one of the deepest basins (max. 248
11 m) within the Baltic Proper (Fig. 2). The gravity core (GC) 303600 (length 377 cm) was
12 collected in the Gotland Basin ($56^{\circ}55.02\text{ N}$, $19^{\circ}19.98\text{ W}$) at 175 m water depth during a cruise
13 onboard the *R/V “Prof. Albrecht Penck”* in July 2009. The multicore (MUC) P435-1-4
14 (length 51.5 cm) was also collected in the Gotland Basin ($56^{\circ}57.94\text{ N}$, $19^{\circ}22.21\text{ E}$) at 178 m
15 water depth during cruise P435 onboard the *R/V “Poseidon”* in June 2012. The dating of the
16 MUC and the brackish section of the GC was based on an age model, obtained by high
17 resolution ^{14}C dating of benthic foraminifera (Warden, 2017; Warden et al., 2017), which
18 allowed us to date the MUC (as calculated kilo years before present, cal. kyr BP, and the
19 corresponding AD) and the GC (as cal. kyr BP) back to 230 cm depth, which corresponds to
20 ca. 7200 cal. yr BP.

21 The GC was cut in two halves and sub-sampled at high resolution with 1 cm slices
22 from 0–237 cm and 2 cm slices from 237–377 cm. During the procedure depth 81–82 cm and
23 187–188 cm were missed. The MUC was sub-sampled at 0.5 cm resolution. The sediments
24 obtained were freeze-dried and grounded before further analysis.

25 **2.2 Elemental and stable isotope analysis**

26 Sub-samples were taken from the GC sediment slices for determination of the total organic
27 carbon (TOC) content at IOW and for the analysis of bulk stable nitrogen isotopes ($\delta^{15}\text{N}$) at
28 NIOZ. The total carbon (TC) content of the sediments of the MUC and GC was measured by
29 using an EA 1110CHN analyzer from CE Instruments, while a Multi EA- 2000 Elemental
30 Analyzer (Analytic, Jena, DE) was employed to determine the total inorganic carbon (TIC).
31 The TOC content was calculated as the difference between TC and TIC and expressed in

1 wt.%. The $\delta^{15}\text{N}$ was analyzed in duplicate on a Thermo Finnigan Delta Plus isotope ratio
2 mass spectrometer (irmMS) connected to a Flash 2000 elemental analyzer (Thermo Fisher
3 Scientific, Milan, Italy). Precision of the isotopes analysis was 0.2% for nitrogen
4 measurements.

5 **2.3 Lipid extraction and analysis**

6 All slices from the MUC and alternating slices from the GC were extracted and analyzed for
7 their HG content and distribution. Extraction was performed using an Accelerated Solvent
8 Extractor (ASE 200, DIONEX; 100°C and 7.6×10^6 Pa) with a mixture of dichloromethane
9 (DCM): methanol (MeOH) (9:1, v:v), to obtain a total lipid extract (TLE), which was dried
10 under a flow of N₂. TLE was re-dissolved by sonication (10 min) in DCM/MeOH (1:1, v:v)
11 and aliquots were taken and dried under a flow of N₂. These aliquots were dissolved in
12 hexane, isopropanol and water (72:27:1, v:v:v) and filtered through a 0.45 µm regenerated
13 cellulose syringe filter (4 mm diameter; Grace Alltech). Samples were analyzed by using a
14 HPLC-triple quadrupole MS in multi-reaction monitoring (MRM) mode as described by Bale
15 et al. (2015). For the analysis, an Agilent (Palo-Alto, CA, US) 1100 series HPLC with a
16 thermostat-controlled auto-injector was employed coupled to a Thermo TSQ Quantum EM
17 triple quadrupole MS equipped with an Ion Max source with ESI probe. The MRM method
18 specifically targets C₅ and C₆ HGs with alkyl chains containing 26 and 28 carbon atoms (Bale
19 et al., 2015). HGs were quantified as the integrated peak area per g of TOC (response units,
20 r.u. gTOC⁻¹). The r.u. gTOC⁻¹ values were simplified for practical purpose by dividing them
21 by 1×10^{10} . For the MUC, 30% of the samples were re-analyzed as duplicates; the calculated
22 relative standard deviation was on average 5.3%. For all GC samples we performed the
23 HPLC/MS² analysis twice; in this case the calculated relative standard deviation was on
24 average 12.4%.

25 A selected number of samples was analyzed in full scan mode using an Ultra High
26 Pressure Liquid Chromatography-High Resolution Mass Spectrometry (UHPLC-HRMS)
27 method (Moore et al., 2013) as follows: we used an Ultimate 3000 RS UHPLC, equipped with
28 thermostatted auto-injector and column oven, coupled to a Q Exactive Orbitrap MS with Ion
29 Max source with heated electrospray ionization (HESI) probe (Thermo Fisher Scientific,
30 Waltham, MA). Separation was achieved on an Acquity UPLC BEH HILIC column (150 x
31 2.0 mm, 2.1 µm particles, pore size 12 nm; Waters, Milford, MA) maintained at 30 °C.
32 Elution was achieved with (A) hexane-propanol-formic acid-14.8 mol L⁻¹ aqueous NH₃
33 (79:20:0.12:0.04, v/v/v/v) and (B) propanol water-formic acid-14.8 mol L⁻¹ aqueous NH₃

1 (88:10:0.12:0.04, v/v/v/v) starting at 100% A, followed by a linear increase to 30% B at 20
2 min, followed by a 15 min hold, and a further increase to 60% B at 50 min. Flow rate was 0.2
3 ml min⁻¹, total run time was 70 min, followed by a 20 min re-equilibration period. Positive ion
4 ESI settings were: capillary temperature, 275°C; sheath gas (N₂) pressure, 35 arbitrary units
5 (AU); auxiliary gas (N₂) pressure, 10 AU; spray voltage, 4.0 kV; probe heater temperature,
6 275°C; S-lens 50 V. Target lipids were analyzed with a mass range of m/z 350–2000
7 (resolution 70,000 ppm at m/z 200), followed by data-dependent tandem MS² (resolution
8 17,500 ppm), in which the ten most abundant masses in the mass spectrum were fragmented
9 successively (normalized collision energy, 35; isolation width, 1.0 m/z). The Q Exactive was
10 calibrated within a mass accuracy range of 1 ppm using the Thermo Scientific Pierce LTQ
11 Velos ESI Positive Ion Calibration Solution. During analysis dynamic exclusion was used to
12 temporarily exclude masses (for 6 s) in order to allow selection of less abundant ions for MS2.

13 A number of indices have been suggested to express correlation between the
14 distribution of HGs and growth temperature (Bauersachs et al., 2009a, 2014b, 2015). We
15 examined our data using two such indices, the HDI₂₆ and the HDI₂₈ (heterocyst diol index of
16 26 and 28 carbon atoms, respectively), defined as follows:

$$\text{HDI}_{26} = \frac{\text{HG}_{26} \text{ diol}}{\text{HG}_{26} \text{ keto} - \text{ol} + \text{HG}_{26} \text{ diol}} \quad (1)$$

$$\begin{aligned} \text{HDI}_{26} &= 0.0224 \times \text{SWT} + 0.4381; r^2 \\ &= 0.93 \end{aligned} \quad (2)$$

$$\text{HDI}_{28} = \frac{\text{HG}_{28} \text{ diol}}{\text{HG}_{28} \text{ keto} - \text{ol} + \text{HG}_{28} \text{ diol}} \quad (3)$$

$$\begin{aligned} \text{HDI}_{28} &= 0.0405 \times \text{SWT} + 0.0401; r^2 \\ &= 0.70 \end{aligned} \quad (4)$$

17 SWT = surface water temperature. These SWT calibrations have been determined in a study
18 of a freshwater lake (Lake Schreventeich, Kiel, Germany; Bauersachs et al., 2015).

19

20 2.4 Data analysis

21 Principal component analysis (PCA) was performed with the R software package for
22 statistical computing, to test the variation observed in the HGs distribution.

1 **3 Results**

2 **3.1 Sediment core characteristics**

3 The basin has experienced periodical anoxic bottom waters, which resulted in the alternating
4 deposition of laminated and homogeneous sediments (Fig. 3; see also Andrén et al. (2000)).
5 The sediments of the MUC represent almost 1000 yr of sedimentation and comprise the
6 MoWP (~0–11 cm depth, corresponding to ~2012–1950 AD or -0.06 to 0 cal kyr BP), the
7 LIA (~12–41 cm, corresponding to ~1950–1260 AD or ~0.1–0.7 cal kyr BP) and almost the
8 entire MWP (~42–52 cm, corresponding to ~0.7–0.9 cal kyr BP). The upper part of the GC
9 overlaps with the deeper part of the MUC (i.e. ~0 to 17 cm depth in the GC roughly
10 corresponds to ~35 to 52 cm of the MUC). The upper part of the GC covers the initial phases
11 of the LIA (until ca. 6 cm, ~0.6 cal kyr BP), the complete Littorina Sea and Ancylus Lake
12 stages, down to part of the Yoldia Sea stage.

13 **3.2 Abundance and distribution of HGs**

14 In total 104 sediment horizons of the MUC and 153 horizons of the GC were analyzed for C₆
15 and C₅ HGs with alkyl chains with 26 and 28 carbon atoms using HPLC-triple quadrupole
16 MS in multi-reaction monitoring (MRM) mode as described by Bale et al. (2015). Bauersachs
17 et al. (2017) have recently analyzed the HGs of eight representative heterocystous
18 cyanobacterial strains isolated from the Baltic Sea and the six C₆ HGs targeted in our study
19 form by far the majority (i.e. 97.7-100%) of the HGs of these strains. HGs with longer alkyl
20 chains were not detected, suggesting that, at least for the brackish phase, our analysis method
21 will provide a proper view of changes in the overall HG distribution.

22 C₅ HGs were not detected at all, but the targeted C₆ HGs were present in all samples
23 of both cores. The C₆ HGs detected in this study were: 1-(O-hexose)-3,25-hexacosanediol
24 (C₂₆ diol HG; see Fig. 1 for structures); 1-(O-hexose)-3-keto-25-hexacosanol (C₂₆ keto-ol
25 HG); 1-(O-hexose)-3,27-octacosanediol (C₂₈ diol HG); 1-(O-hexose)-3-keto-27-octacosanol
26 (C₂₈ keto-ol HG); 1-(O-hexose)-3,25,27-octacosanetriol (C₂₈ triol HG); 1-(O-hexose)-27-keto-
27 3,25-octacosanediol (C₂₈ keto-diol HG). A selected number of samples from the brackish
28 phase was also analyzed in full scan mode to check for the presence of HGs with longer alkyl
29 side chains but these were not encountered (Table 2). The HG distribution obtained using this
30 method was comparable to that obtained with the HPLC-triple quadrupole MS method.

31 The distribution of the six quantified HGs changed substantially with depth (Fig. 4).
32 The C₂₆ diol HG was the dominant component, accounting for ~50 to 95% of the HGs in the

1 sediments recording the brackish phase of the basin. In the sediments deposited during the
2 Ancylus Lake and Yoldia phase (i.e. below 213 cm of the GC) the fractional abundance of the
3 C₂₆ diol HG was more variable, reaching only 20–30% at some discrete depths. In the
4 sediments deposited during the brackish phase the fractional abundance of all keto HGs (i.e.,
5 C₂₆ keto-ol HG, C₂₈ keto-ol HG and C₂₈ keto-diol HG) diminished with increasing depth,
6 roughly from 3–15% to <2% (Fig. 4b). In the sediments deposited during the Ancylus Lake
7 and Yoldia Sea phase, however, their fractional abundance showed more variation and in
8 general it increased and reached ~10–40% at some specific depths. The fractional abundance
9 of the C₂₈ diol HG remained steady for most of the sediments deposited during the brackish
10 phase (~10% on average), although slightly increased values occurred in the oldest part of the
11 brackish section, up to ~15% (Fig. 4b). In the Ancylus Lake and Yoldia Sea section the
12 fractional abundance of the C₂₈ diol HG was higher, with values sometimes reaching almost
13 60%, but also more variable. The fractional abundance of the C₂₈ triol HG was <2% for most
14 of the sediments deposited during brackish phase, with the exceptions of the shallower (8–
15 16%) and the deeper part, close to the boundary with the freshwater phase (3–9%). In the
16 Ancylus Lake and Yoldia Sea sections the relative abundance of the C₂₈ triol HG generally
17 remained <2%, although it was between 3–11% in several horizons in the deeper part (Fig.
18 4b). For the Ancylus Lake and Yoldia Sea section we did not check the general distribution of
19 the HGs and, therefore, cannot exclude that HGs with alkyl chains >28 carbon atoms occur
20 during these intervals.

21 The C₆ HG abundance (sum of the six C₆ HGs; hereafter referred to as HG abundance)
22 profile showed four peaks in the first 8 cm of the MUC of respectively 144, 82, 117 and 69
23 r.u. gTOC⁻¹ (Fig. 3a). After this last peak, the abundance of the HGs decreased substantially
24 by a factor ~30 in some cases (i.e., ~5 r.u. gTOC⁻¹) and remained at this level with increasing
25 depth over the whole of the MUC (Fig. 3a).

26 The HG abundance in the upper part of the GC (up to ~11 cm) was 3 to 6 times higher
27 (7 to 18 r.u. gTOC⁻¹) than that recorded in the corresponding fraction of the MUC (2 to 4 r.u.
28 gTOC⁻¹). At ~17 cm of the GC, which is equivalent to ~52 cm or the bottom of the MUC, the
29 abundance were in the same order of magnitude (4 to 5 r.u. gTOC⁻¹). Between ~25 and 213
30 cm depth (~1.3–7.1 cal kyr BP) the abundance of the HGs decreased substantially further by a
31 factor of ca. 6 to 10, with the exception of several small peaks at discrete depths (respectively,
32 ~5 r.u. gTOC⁻¹ at ~35 cm; ~4 r.u. gTOC⁻¹ at ~53 cm, at ~92 cm and at ~108 cm; ~3 r.u.
33 gTOC⁻¹ at ~188 cm). Deeper in the core (213–375 cm; i.e. the Ancylus Lake and Yoldia
34 phase) the abundance of the HGs was even lower (Fig. 3a).

1 **3.3 Principal component analysis of the HG distribution**

2 The variation observed in the HG distribution in the sediments was examined by applying a
3 principal component analysis (PCA) to the fractional abundances of the six HGs (Fig. 5). The
4 first two principal components (PCs) explained most of the variation observed, accounting for
5 47 and 29% of the variance, respectively (Fig. 5a). The first principal component (PC1)
6 showed a positive loading of all keto HGs and of the C₂₈ triol HG. Specifically, the C₂₆ keto-
7 ol HG and the C₂₈ keto-diol HG had the most positive loading (Fig. 5a). The C₂₆ diol HG was
8 the only component showing a negative loading in PC1; the C₂₈ diol HG did not show any
9 loading on PC1. PC2 is primarily determined by the positive loadings of the C₂₈ diol and
10 keto-ol HGs, whereas all other HGs had negative loadings on PC2.

11 Figure 5b shows the scores of all analyzed sediment horizons on PC1 and PC2, which
12 reveals clearly defined different signatures. The brackish phase sediments all scored
13 negatively or just above zero on PC2. However, the score on PC1 was more variable; the
14 MoWP sediments scored most positively on PC1, whereas the pre-MoWP brackish sediment
15 scored less positive on PC1, which is due to the higher fractional abundances of the C₂₆ keto-
16 ol and C₂₈ keto-diol HGs in the MoWP sediments. The remaining sediments of the Ancylos
17 Lake I and Yoldia Sea phase all scored positively on both PC1 and PC2 and therefore
18 distinctly from the brackish phase sediments but also showed much more variability. The
19 sediments of the Ancylos Lake transitional phase II (filled triangles in Fig. 5b) plotted much
20 closer to those of the brackish phase with some data points with similar PC1 and PC2 values.
21

22 Figure 4 shows the variation of the scores on PC1 and PC2 with depth. The sediments
23 of the MUC exhibited a decreasing trend in PC1 with increasing depth, caused by the
24 reduction in the fractional abundance of the positively scoring keto HGs, in favor of the
25 negatively scoring C₂₆ diol (Fig. 4a). For the GC (Fig 4b), the PC1 scores varied between -2
26 and -1, from the top up to 213 cm depth (i.e. the brackish phase), consistent with the
27 dominance of the C₂₆ diol HG in this section. At greater depth (i.e. the Ancylos Lake and
28 Yoldia Sea phases) large variations in the score of PC1 were observed (Fig. 4b). Scores were
29 mostly positive; negative PC1 scores were only found at three discrete depths, i.e. 239, 303
30 and 343 cm. The generally positive score in these phases highlights the greater contribution of
31 HGs other than C₂₆ diol HG. The PC2 score of the sediments of the MUC was constantly
32 around -1, (Fig. 4a). In the GC, PC2 was close to zero during the brackish water phase (Fig.
33 4b). In the sediments of the Ancylos Lake and Yoldia Sea phases the PC2 score was generally

1 positive, clearly influenced by the higher fractional abundance of positively scoring C₂₈ diol
2 and C₂₈ keto-ol HGs, but variable.

3 **4 Discussion**

4 This study investigates the presence of HGs in the recent sedimentary record of the Baltic Sea
5 and represents the first attempt to relate them with the recurring anoxic events that took place
6 in the basin during the Holocene as well as the ongoing increase in cHAB over the last 60
7 years. In our data set we recognized various phases, characterized by different distributions of
8 HGs (cf. Figs. 4 and 5b). Here these records and their implications for the heterocystous
9 cyanobacterial community composition are discussed.

10 **4.1 The distribution of HGs**

11 The composition of HGs in cyanobacteria is known to be related to their taxonomy
12 (Bauersachs et al., 2009a, 2014a, Gambacorta et al., 1995, 1998; Schouten et al., 2013;
13 Wörmer et al., 2012). Hence we compared the distribution of the HGs observed in our
14 sedimentary record of the Baltic Sea with the HGs produced *in vitro* by different
15 heterocystous cyanobacterial species.

16 **4.1.1 Brackish sediments**

17 Firstly, the most recent sediments (MoWP, <11 cm depth of MUC) were compared with
18 species that thrive in the modern Baltic Sea (Table 1). The recurring late summer (July-
19 August) cHABs of the Baltic are dominated by the taxa *Nodularia spumigena*,
20 *Aphanizomenon flos-aquae* and, to a minor extent, by *Anabaena* spp. and other species from
21 the order *Nostocales*, family *Nostocaceae* (Hajdu et al., 2007; Hällfors, 2004; Kanoshina et
22 al., 2003; Karjalainen et al., 2007; Sivonen et al., 2007; Celepli et al., 2017). While the
23 *Nodularia* genus is usually prevalent, changes in the composition of the community have been
24 observed from the early to the late stage of the cHAB and from one year to another, resulting
25 in a large variation of its features over time (Finni et al., 2001; Hajdu et al., 2007; Kahru et al.,
26 1994; Wasmund, 1997). A recent extensive meta-omics study revealed that in the Baltic
27 proper (the predominant area for cHABs) 69% of the heterocystous cyanobacteria belong
28 to *Aphanizomenon*, 23% to *Anabaena*, and 8% to *Nodularia* (Celepli et al., 2017).

29 The HG distribution in the MoWP sediment, with the C₂₆ diol as the dominant HG
30 (Fig. 4a, summarized in Table 1), agrees well with the HG distribution in cultures of
31 *Nodularia*, *Aphanizomenon* and *Anabaena* as well as other members of the *Nostocaceae*

1 family (Table 1), including those that have been isolated from the Baltic (Bauersachs et al.,
2 2009a, 2017). These cultures generally also synthesized minor amounts of the C₂₆ keto-ol HG,
3 as was seen in the MoWP sediments. The C₂₈ diol, present in trace amounts in the MoWP
4 sediments, was found in varying amounts in the *Nodularia*, *Aphanizomenon* and *Anabaena*
5 cultures. Even between different strains of the same species, amounts present were highly
6 variable from a dominant component to not detected (Table 1). The C₂₈ keto-ol, C₂₈ triol and
7 C₂₈ keto-diol HGs were minor components in the MoWP sediment. While not produced
8 consistently across the *Nodularia*, *Aphanizomenon* and *Anabaena* cultures, they were found in
9 certain strains, generally as trace or minor components, in agreement with the distribution in
10 the sediment (Table 1). It is possible, however, that the presence of the C₂₈ triol HG in the
11 MoWP sediments may be linked to the presence of the genus *Calothrix* (cf. Table 1), which is
12 commonly found in the rocky seabed of the basin (Sivonen et al., 2007).

13 Overall, the distribution of the HGs observed in the MoWP sediments was in good
14 agreement with the HG distribution of the family *Nostocaceae* (Table 1), which fits with the
15 reported dominance of members of this family during the summer cHABs of the Baltic.
16 Furthermore, the HG distribution remained relatively constant throughout the MoWP
17 sediments (Fig. 4a), suggesting that overall the community composition of heterocystous
18 cyanobacteria in the Baltic Sea has remained stable during the last ~60 years.

19 The HG distribution in the sediment from the pre-MoWP brackish phase (i.e. from the
20 Aencylus Lake-Littorina Sea (AL-LS) transition to the start of the MoWP) reconstructed in this
21 study was similar to that of the MoWP, although the C₂₆ diol and the C₂₈ diol were present in
22 a greater fractional abundance (Table 1; Fig. 4). The other four HGs were either minor or
23 occurred in traces. Although often absent, a number of *Nostocaceae* strains have been found
24 to contain the C₂₈ diol (Table 1), and in one *Anabaena* sp. strain (CCY9402) it was found to
25 be the dominant HG (Bauersachs et al., 2009a). The increased proportion of the C₂₈ diol
26 through the pre-MoWP brackish phase suggests there was a somewhat different
27 cyanobacterial community composition than during the MoWP, although most probably still
28 dominated by cyanobacteria belonging to the family *Nostocaceae*. The HG distribution
29 remained relatively constant from the establishment of the brackish phase to the MoWP (Fig.
30 4), which suggests that the cyanobacterial community of the Baltic did not undergo major
31 changes from the AL-LS transition to the MoWP and remained dominated by cyanobacteria
32 belonging to the family *Nostocaceae*.

33 **4.1.2 The Aencylus Lake sediments**

1 The Ancylus Lake phase displayed a distinct HG distribution from the brackish phase (Fig.
2 4b; summarized in Table 1). The C₂₈ diol was often dominant and both the C₂₆ and C₂₈ keto-ol
3 were present in a higher proportion than during the brackish phase. This is most evident for
4 the Ancylus Lake phase I and the middle section (ca. 230-210 cm) of the Ancylus Lake phase
5 II. Yet, at the first (ca. 250-230 cm) and last part (ca. 210-193 cm) of the Ancylus Lake
6 transitional phase II, the HG distribution is more similar to the one observed in the brackish
7 phase (Fig. 4b). This is also evident from the PCA analysis with more negative values for PC1
8 and PC2 at those depths (Figs. 4b and 5b). The AL-LS transition did not happen instantly
9 (Borgendahl and Westman, 2007; Emeis et al., 1998; Gustafsson and Westman, 2002;
10 Hyvarinen, 1984) and probably the sediment intervals showing a brackish-like distribution of
11 the HGs correspond to weak pulses of marine water that might have occasionally entered the
12 basin already during the Ancylus Lake transitional phase II and consequently influenced the
13 overall distribution of the HGs (Fig. 4b). This final stage of this transition is also evident from
14 the lithology and TOC profile (Fig. 3c).

15 When the Baltic evolved from a freshwater lake into a brackish semi-enclosed basin, it
16 experienced an increase in salinity from fresh to values of 10–15 ‰ (Gustafsson and
17 Westman, 2002). The observed changes in the HG distribution over the AL-LS transition
18 suggest that this change from freshwater to brackish resulted in a different cyanobacterial
19 species composition and hence a different HG distribution. Indeed, several freshwater species
20 have been found to contain a HG distribution dominated by the C₂₈ diol (Table 1), including
21 *Cyanospira rippkae* (Soriente et al., 1993), *Tolypothrix tenuis* (Gambacorta et al., 1998) and
22 *Aphanizomenon aphanizomenoides* (Wörmer et al., 2012), although we emphasize that we did
23 not analyze HGs with C₂₈₊ alkyl chains for this stage and, therefore, cannot exclude the
24 contributions of cyanobacteria producing such extended HGs. Alternatively, an increased
25 influx of soil organic matter during the Ancylus Lake phase could be responsible for the
26 distributional HG changes. However, since HG lipids contain an attached sugar moiety, we
27 feel it is unlikely that HGs produced in soil will make it to the sediments of the Baltic Sea
28 since they would be exposed extensively to oxygen during transport and only relatively stable
29 components such as lignin, wax lipids, and branched GDGTs will likely survive this transport
30 to the middle of the Baltic Sea where our core was taken.

31 For *Nodularia spumigena*, the most abundant heterocystous cyanobacterium in the
32 present Baltic, its basic physiological features, such as growth, production of the toxin
33 nodularin and differentiation of heterocysts are substantially affected at extreme salinities
34 (Mazur-Marzec et al., 2005; Moisander et al., 2002). This is thought to be the predominant

1 reason why *Nodularia* blooms only occur within a certain salinity range (i.e. 7–18‰) in
2 nitrogen-deficient waters (Mazur-Marzec et al., 2005). This would imply that during the
3 Ancylus Lake phase the low salinity was limiting the growth of *Nodularia* sp.. Other
4 heterocystous cyanobacteria such as *Anabaena* and *Aphanizomenon* may be better adapted to
5 freshwater conditions.

6 **4.1.3 Yoldia Sea sediments**

7 Also for the Yoldia Sea sediments a high variability is observed in the HG distribution (Figs.
8 4b, 5b). The most distinct feature is the relatively high fractional abundance of the C₂₈ diol
9 HG, which reaches sometimes 50%, the highest value recorded for all sediments. The Yoldia
10 Sea phase was a relatively short period when a connection with the sea was established and
11 waters may have become brackish. Nevertheless, the HG distribution is not at all similar to
12 that of the brackish phase.

13 **4.1.4 Does the distribution of the fossil HGs records a paleotemperature signal?**

14 As a consequence of the retreat of the ice sheet and the inlet of the sea water through the
15 Danish straits, there was an increase of water temperature during the AL–LS transition
16 (Björck, 1995). It is possible that this increase in water temperature could have been
17 responsible for the changes in the HG distribution, as growth temperature has been reported to
18 affect the distribution of the HGs in cyanobacteria belonging to the order *Nostocales*
19 (Bauersachs et al., 2009a, 2014b, 2015). Specifically, increasing temperature positively
20 correlated with increasing relative proportions of HG diols over HG keto-ols. In our record,
21 the ratio of diols to keto-ols increased from the Ancylus Lake towards the brackish phase
22 (Fig. 4b), which would be in agreement with the higher SWTs during the brackish phase.
23 However, when the HG proxies are used to estimate SWT based on the proxy calibrations
24 from a lake (Eq. 1–4), the predicted temperatures are somewhat unrealistic. For the brackish
25 phase the HDI₂₆ and HDI₂₈ values vary between 0.96–1.00 and 0.95–1.00, translating in
26 average SWT of ca. 24 and 23°C, respectively. This is too high, even for summer
27 temperatures when the cHABs occur (Kanoshina et al., 2003). TEX₈₆-derived summer
28 temperatures (Kabel et al., 2012; Warden et al., 2017) do not exceed 17.5°C (Fig. 3d).
29 Application of the HG-based calibrations in this setting assumes that salinity has no impact
30 since they have been established for a freshwater lake (Bauersachs et al., 2015). For the
31 Ancylus Lake and Yoldia Sea phases the HDI₂₆ and HDI₂₈ values are highly variable and
32 range between 0.52–1.00 and 0.00–0.99, translating in average SWTs of ca. 20 and 17°C,

1 respectively. This is lower than observed for the brackish phase but also seems too high.
2 Apparently, cyanobacterial species composition exerts an important control on the HG
3 distribution in such a way that the HGs are not able to predict accurate temperatures in the
4 brackish/freshwater system of the Baltic. Cultivation experiments with HG-producing strains
5 isolated from the Baltic Sea (see Table 1) at varying temperatures may improve HG
6 palaeothermometry of Baltic Sea sediments.

7 **4.2 The abundance of HGs**

8 **4.2.1 Is HG abundance a good measure for cHABs and anoxic events?**

9 In the Baltic the occurrence of summer cHABs has intensified since the 1950s (Kabel et al.,
10 2012; Poutanen and Nikkilä, 2001). Yet, due to the spatial patchiness and inter-annual
11 variability, it has proven difficult to recognize a clear trend of the cHABs at the scale of the
12 entire Baltic (Finni et al., 2001; Kahru and Elmgren, 2014; Pitarch et al., 2016; Wasmund and
13 Uhlig, 2003). However, the general interest towards these events has led to intensified
14 research (see Finni et al., 2001; Kahru and Elmgren, 2014; Kutser et al., 2006 among others)
15 and to the establishment of the Baltic Marine Environment Protection Commission
16 (HELCOM) in 1992 to monitor this phenomenon. Disparate indices and parameters have been
17 employed to describe and quantify cHABs over time, and were applied in the different areas
18 of the Baltic, which are biogeochemically heterogeneous and display distinct seasonal
19 dynamics (Kahru, 1997; Kahru et al., 2007; Kahru and Elmgren, 2014; Kononen, 1992;
20 Kutser et al., 2006; Pitarch et al., 2016; Wasmund and Uhlig, 2003). The methods employed
21 and the frequency of the sampling campaigns have improved in the recent past, reducing the
22 inaccuracy associated to previous sampling methods and measurements (Hansson and Öberg,
23 n.d.; Kahru, 1997; Kahru and Elmgren, 2014; Wasmund and Uhlig, 2003). However, intrinsic
24 limitations of the techniques in use may still cause difficulties when comparing measurements
25 from different years, even within the same time series (Finni et al., 2001; Kahru, 1997; Kahru
26 and Elmgren, 2014).

27 Here, the HG abundance over the past ~30 years (i.e. 2012–1979 of the MoWP),
28 recorded within the first ~7 cm of the MUC are discussed in comparison with a time series of
29 the cHABs episodes relative to the Eastern Gotland Basin (Fig. 6), whose intensity is
30 expressed as the frequency of cyanobacteria accumulation (FCA) (Kahru and Elmgren, 2014).
31 FCA is determined by ocean color satellite data and expresses the frequency of the occurrence
32 of cHABs in July-August using 1 km² pixels (Kahru et al., 2007). Kahru and Elmgren (2014)
33 reported prominent cHABs in the early 1980s, in the period 1990–1996 and again from 1999

until 2008, with the interval 2005–2008 recording the highest FCA percentages, whilst with relevant inter-annual changes of the areal extent (Kahru, 1997; Kahru et al., 1994, 2007; Kahru and Elmgren, 2014). The HG lipid biomarker abundance profile from our sampling site was overall in reasonable agreement with the FCA measurements (Fig. 6). However, it failed to record the intense cHABs of the early 1980s, and there is a mismatch of one or two years in recording the start of the strong cHABs recorded at the end of the same decade (Kahru and Elmgren, 2014). Furthermore, this comparison is complicated by a certain degree of uncertainty in the age model of the sedimentary record. Moreover, the intrinsic temporal and spatial variability of the cHABs in the modern Baltic Sea, together with the difficulties encountered in the attempt of creating a consistent long time series that combines FCA data from multiple satellite sensors may provide an explanation for the discrepancies observed (Kahru and Elmgren, 2014; Wasmund and Uhlig, 2003).

We observed multiple peaks of the HGs absolute abundance in the MoWP section of the MUC core (≤ 11 cm depth), which reached ~ 50 – 150 r.u. gTOC $^{-1}$. Below this in the LIA section, the HG abundance declined sharply to < 10 r.u. gTOC $^{-1}$ (Fig. 3a). This decline may be expected given that the MoWP is characterized by higher summer surface temperature (Fig. 3d), increased organic matter deposition, and more frequent anoxic events than the LIA phase (Kabel et al., 2012), all conditions that lead to increased cHABs. Furthermore, the cooler LIA experienced more oxygenated bottom water, which may have affected HG preservation (see also below). However, a substantially increased HG abundance was not observed below the LIA in the MWP section of the MUC core (Fig. 3a). Similar to the MoWP period, the MWP was characterized by higher summer temperatures (Fig. 3d) and increased stratification of the water column that would favor bottom anoxia and, presumably, the occurrence of cHABs. The top of the GC also records the LIA–MWP transition (Fig. 3). Here, the HGs abundance reached ~ 10 – 18 r.u. gTOC $^{-1}$ at < 30 cm depth, which is up to 4 times higher than the HGs abundance observed in the MUC for the same period. This discrepancy between the HGs records in the two related cores is puzzling. After the MWP, HG abundance declined to ≤ 5 r.u. gTOC $^{-1}$ during the remaining part of the brackish phase, as recorded in the GC (Fig. 3a), with only a minor increase of the HG concentration during the periods when summer temperature was higher and the Baltic Sea was stratified, resulting in bottom water anoxia (Fig. 3; e.g. during the Holocene thermal maximum).

Based on these data from the Baltic Sea, it is not possible to confidently couple the HG abundance record directly to cHAB occurrences and anoxic events in the past. Several

1 factors are thought to affect this relationship. Firstly, it is possible that the occurrence of
2 cHABs varied over time. In the shallow part of both sediment cores, HGs absolute abundance
3 was generally high, but it started declining with increasing depth, independently from other
4 factors (Fig. 3). This might suggest that cHABs were less common and intense in the past
5 brackish Baltic Sea, even at times of warmer and more stratified conditions. Secondly, the
6 succession of oxic/anoxic bottom water conditions may impact the preservation efficiency of
7 HGs. Such successions took place in the Baltic Sea during the entire Holocene as is evident
8 from the alternation of dark-laminated with light-homogeneous sections in the sedimentary
9 record (Kabel et al., 2012). In the shallow part of both sediment cores, the high absolute
10 abundance of HGs coincided with dark-laminated sediment phases; low HGs on the contrary,
11 concurred with light-homogeneous phases. In contrast, in the deeper part of the section this
12 correspondence was lost. Finally, the generally declining trend of the HGs absolute
13 abundance in the shallow sediments might also be due to anaerobic breakdown of the HGs. A
14 decline of lipid biomarkers with depth has been documented before in anoxic Black Sea
15 surface sediments (Sun and Wakeham, 1994). This process would be seemingly in contrast
16 with previous indications of a high preservation potential of the HGs in ancient marine and
17 lacustrine anoxic sediments (Bauersachs et al., 2010), but it should be realized that even in the
18 older Baltic Sea sediments HGs are still detected. Apparently, even if diagenesis is occurring,
19 it does not result in complete destruction of HGs.

20 The HG results seem to partly contrast an earlier study that, based on fossil pigment
21 records, suggested that cHABs have been recurring simultaneously with the mid-Holocene
22 anoxic events (Funkey et al., 2014). However, this study used carotenoids (i.e. zeaxanthin and
23 echinenone) that are not entirely specific for cyanobacteria and are certainly not limited to
24 nitrogen-fixing cyanobacteria, as opposed to the highly specific HGs that were used here. For
25 example, zeaxanthin is also produced by *Synechococcus*, the dominating unicellular
26 cyanobacterial species in the Baltic Sea (Celepli et al., 2017). Furthermore, in this
27 environment of highly variable sediment redox conditions the effect of diagenesis should be
28 considered. Carotenoids are amongst the most unstable organic biomarkers because of their
29 very labile conjugated system of double bonds. Changes in redox conditions of bottom and
30 sediment pore waters will thus have a major effect on the concentration of carotenoids and
31 this may explain the enhanced concentration of carotenoids in the mid-Holocene TOC-
32 enriched sections (Funkey et al., 2014).

33 **4.2.2 Changing abundance of the HGs over the AL-LS transition**

1 The general down-core decrease in the HGs abundance throughout the brackish phase is
2 continued into the Ancylus Lake and Yoldia Sea phases, where the HG abundance is at least
3 an order of magnitude lower than in the first part of the brackish phase (Fig. 3a). The lower
4 HG abundance in the Ancylus Lake and Yoldia Sea phases, relative to the brackish phase,
5 could indicate that N₂-fixing cyanobacteria were much less abundant during this freshwater
6 phase. Indeed, further evidence for a lower abundance of diazotrophic phytoplankton during
7 the Ancylus Lake and Yoldia Sea phases comes from the record of δ¹⁵N values (Fig. 3b).
8 During these phases the δ¹⁵N values are 4–6 ‰, indicating that most of the phytoplankton
9 community was relying on ammonium or nitrate as nitrogen sources rather than atmospheric
10 nitrogen (Bauersachs et al., 2009b; Emerson and Hedges, 2008). When other forms of
11 nitrogen are abundant the energetically expensive N₂ fixation becomes disadvantageous
12 (Arrigo, 2005; Capone et al., 2005; Karl et al., 1997). At the start of the LS phase, δ¹⁵N values
13 drop to 1–3‰ (Fig. 3b), a range expected when N₂-fixing cyanobacteria contribute
14 substantially to primary production (Bauersachs et al., 2009b; Rejmánková et al., 2004;
15 Zakrisson et al., 2014), and remained in this range.

16 As discussed above, the salinity change from a freshwater lake to a brackish sea may
17 have had a significant effect on the heterocystous cyanobacterial composition in the Baltic. This
18 environmental change may have also been a cause of the increased abundance of
19 heterocystous cyanobacteria. Another environmental factor change that could have promoted
20 increased blooming of heterocystous cyanobacteria is the increase in water temperature over
21 the AL–LS transition (Björck, 1995). Temperature is a crucial factor influencing the growth
22 rate and other metabolic features of free-living heterocystous cyanobacteria (Bauersachs et al.,
23 2014b; Kabel et al., 2012; Mazur-Marzec et al., 2005; Staal et al., 2003). In the modern Baltic
24 Sea a minimum temperature of 16°C is considered essential to initiate cHABs during summer,
25 when other crucial factors like low DIN/DIP ratio, calm winds and high irradiance occur
26 simultaneously (Kanoshina et al., 2003; Kononen, 1992; Kononen et al., 1996; Paerl, 2008;
27 Wasmund, 1997).

28 It should also be noted, however, that the homogeneous appearance of the sediments
29 and the much reduced TOC content (Fig. 3c) reveals that the water column was generally well
30 mixed and oxygenated during the Ancylus Lake and Yoldia Sea phases, resulting in a higher
31 degradation of organic matter (including HGs) in settling particles and surface sediments. To
32 compensate for this effect all HG concentrations were normalized to TOC content (Fig. 3a).
33 However, it is known that oxic conditions in the sediment result in a decreased preservation of

1 biomarkers relative to TOC (see Sinninghe Damsté et al., 2002). This may also explain in part
2 the lower HG abundance in the Ancylus Lake and Yoldia Sea than in the brackish phase.
3 However, it is noteworthy that no substantial change in the concentration of HGs is observed
4 during the brackish phase when bottom water conditions changed from oxic to anoxic (Fig.
5 3). This suggest that the normalization to TOC content is an effective way to compensate for
6 changing redox conditions of bottom and pore waters. The effect of oxic degradation is
7 probably also not responsible for substantial changes in the distribution of the HGs since they
8 are structurally similar and all contain a relatively labile glycosidic bond, so there is no reason
9 to assume that one HG will degrade faster than another.

10 **Conclusions**

11 The distribution of the six analyzed C₆ HGs in the Baltic sediments from the brackish phases
12 were closely related to those of cultivated heterocystous cyanobacteria of the family
13 *Nostocaceae*. The record also shows that the HGs distribution has remained stable since the
14 Baltic has turned into a brackish semi-enclosed basin ~7200 cal. yrs BP. During the
15 freshwater phase of the Baltic (i.e. the Ancylus Lake phase) and an earlier brackish period
16 (the Yoldia Sea phase) the distribution of the HGs was quite distinct but varied much more
17 than in the subsequent brackish phase. This suggests that the cyanobacterial community
18 adjusted to the different environmental conditions in the basin over this transition. We found
19 that the abundance of HGs dropped substantially down-core, possibly either due to a decrease
20 of the cHABs or during oxic degradation during deposition, resulting in partial destruction of
21 the HGs.

22 In conclusion, it is likely that both salinity and temperature have influenced the
23 abundance and composition of the heterocystous cyanobacterial community of the Baltic
24 since the last deglaciation. The effects of salinity on the synthesis and distribution of HGs
25 would need to be investigated in controlled conditions to be confirmed, as it has been partially
26 done already in the case of temperature. Further studies are also needed to extend the range of
27 heterocystous cyanobacteria species in culture that have been investigated for their HGs
28 content.

29

30 **Acknowledgements**

31 We thank the captain and the crew of the R/V “*Prof. Albrecht Penck*” (cruise July 2009), and
32 of the R/V “*Poseidon*” (cruise June 2012), for their support and assistance in the sampling.

1 We thank Mati Kahru for providing FCA data and three anonymous referees and Prof. Dan
2 Conley for helpful suggestions on an earlier draft of this paper. This project was funded by a
3 grant to JSSD from the Darwin Center for Biogeosciences (project nr. 3012). The work was
4 further supported by funding from the Netherlands Earth System Science Center (NESSC)
5 through a gravitation grant (NWO 024.002.001) from the Dutch Ministry for Education,
6 Culture and Science to JSSD.

7
8

9 **References**

- 10 Adams, D. G.: Heterocyst formation in cyanobacteria, *Curr. Opin. Microbiol.*, 3(6), 618–624,
11 2000.
- 12 Andrén, E., Andrén, T. and Kunzendorf, H.: Holocene history of the Baltic Sea as a
13 background for assessing records of human impact in the sediments of the Gotland Basin,
14 *Holocene*, 10(6), 687–702, doi:10.1191/09596830094944, 2000.
- 15 Andrén, T., Björck, S., Andrén, E., Conley, D. J., Zillén, L. and Anjar, J.: The Baltic Sea
16 Basin, in Central and Eastern European Development Studies (CEEDES), edited by J. Harff,
17 S. Björck, and P. Hoth, pp. 75–97, Springer., 2011.
- 18 Arrigo, K. R.: Marine microorganisms and global nutrient cycles, *Nature*, 437(7057), 349–
19 355, doi:10.1038/nature04158, 2005.
- 20 Bale, N. J., Hopmans, E. C., Zell, C., Lima Sobrinho, R., Kim, J. H., Sinninghe Damsté, J. S.,
21 Villareal, T. A. and Schouten, S.: Long chain glycolipids with pentose head groups as
22 biomarkers for marine endosymbiotic heterocystous cyanobacteria, *Org. Geochem.*, 81, 1–7,
23 doi:10.1016/j.orggeochem.2015.01.004, 2015.
- 24 Bale, N. J., Hopmans, E. C., Schoon, P. L., de Kluijver, A., Downing, J. A., Middelburg, J. J.,
25 Sinninghe Damsté, J. S. and Schouten, S.: Impact of trophic state on the distribution of intact
26 polar lipids in surface waters of lakes, *Limnol. Oceanogr.*, 61(3), 1065–1077,
27 doi:10.1002/lno.10274, 2016.
- 28 Bale, N. J., Villareal, T. A., Hopmans, E. C., Brussaard, C. P. D., Besseling, M., Dorhout, D.,
29 Sinninghe Damsté, J.S. and Schouten, S.: C₅ glycolipids of heterocystous cyanobacteria track
30 symbiont abundance in the diatom *Hemiaulus hauckii* across the tropical north Atlantic.
31 *Biogeosci. Discuss.*, <https://doi.org/10.5194/bg-2017-300>, 2017.
- 32 Bauersachs, T., Compaore, J., Hopmans, E. C., Stal, L. J., Schouten, S. and Sinninghe
33 Damsté, J. S.: Distribution of heterocyst glycolipids in cyanobacteria, *Phytochem.*, 70(17–18),
34 2034–2039, doi:10.1016/j.phytochem.2009.08.014, 2009a.
- 35 Bauersachs, T., Schouten, S., Compaoré, J., Wollenzien, U., Stal, L. J. and Sinninghe Damsté,
36 J. S.: Nitrogen isotopic fractionation associated with growth on dinitrogen gas and nitrate by
37 cyanobacteria, *Limnol. Oceanogr.*, 54(4), 1403–1411, doi:10.4319/lo.2009.54.4.1403, 2009b.

- 1 Bauersachs, T., Hopmans, E. C., Compaore, J., Stal, L. J., Schouten, S. and Sinninghe
2 Damsté, J. S.: Rapid analysis of long-chain glycolipids in heterocystous cyanobacteria using
3 high-performance liquid chromatography coupled to electrospray ionization tandem mass
4 spectrometry, *Rapid Commun. Mass Spectrom.*, 23(9), 1387–1394, doi:10.1002/rcm.4009,
5 2009c.
- 6 Bauersachs, T., Speelman, E. N., Hopmans, E. C., Reichart, G.-J., Schouten, S. and Sinninghe
7 Damsté, J. S.: Fossilized glycolipids reveal past oceanic N₂ fixation by heterocystous
8 cyanobacteria, *Proc. Natl. Acad. Sci. U. S. A.*, 107(45), 19190–19194,
9 doi:10.1073/pnas.1007526107, 2010.
- 10 Bauersachs, T., Compaore, J., Severin, I., Hopmans, E. C., Schouten, S., Stal, L. J. and
11 Sinninghe Damsté, J. S.: Diazotrophic microbial community of coastal microbial mats of the
12 southern North Sea, *Geobiology*, 9(4), 349–359, doi:10.1111/j.1472-4669.2011.00280.x,
13 2011.
- 14 Bauersachs, T., Miller, S. R., van der Meer, M. T. J., Hopmans, E. C., Schouten, S. and
15 Sinninghe Damsté, J. S.: Distribution of long chain heterocyst glycolipids in cultures of the
16 thermophilic cyanobacterium *Mastigocladus laminosus* and a hot spring microbial mat, *Org.*
17 *Geochem.*, 56, 19–24, doi:10.1016/j.orggeochem.2012.11.013, 2013.
- 18 Bauersachs, T., Mudimu, O., Schulz, R. and Schwark, L.: Distribution of long chain
19 heterocyst glycolipids in N₂-fixing cyanobacteria of the order Stigonematales, *Phytochem.*,
20 98, 145–150, doi:10.1016/j.phytochem.2013.11.007, 2014a.
- 21 Bauersachs, T., Stal, L. J., Grego, M. and Schwark, L.: Temperature induced changes in the
22 heterocyst glycolipid composition of N₂ fixing heterocystous cyanobacteria, *Org. Geochem.*,
23 69, 98–105, doi:10.1016/j.orggeochem.2014.02.006, 2014b.
- 24 Bauersachs, T., Rochelmeier, J. and Schwark, L.: Seasonal lake surface water temperature
25 trends reflected by heterocyst glycolipid-based molecular thermometers, *Biogeosciences*,
26 12(12), 3741–3751, doi:10.5194/bg-12-3741-2015, 2015.
- 27 Bauersachs, T., Talbot, H. M., Sidgwick, F., Sivonen, K., and Schwark, L.: Lipid biomarker
28 signatures as tracers for harmful cyanobacterial blooms in the Baltic Sea. *PLoS One*, 12,
29 e0186360, 2017.
- 30 Bianchi, T. S., Engelhaupt, E., Westman, P., Andrén, T., Rolff, C. and Elmgren, R.:
31 Cyanobacterial blooms in the Baltic Sea: Natural or human-induced?, *Limnol. Oceanogr.*,
32 45(3), 716–726, doi:10.4319/lo.2000.45.3.0716, 2000.
- 33 Björck, S.: A review of the history of the Baltic Sea, 13.0–8.0 ka BP, *Quat. Int.*, 27, 19–40,
34 doi:10.1016/1040-6182(94)00057-C, 1995.
- 35 Borgendahl, J. and Westman, P.: Cyanobacteria as a trigger for increased primary
36 productivity during sapropel formation in the Baltic Sea—a study of the Acanthocystis/Litorina
37 transition, *J. Paleolimnol.*, 38(1), 1–12, doi:10.1007/s10933-006-9055-0, 2007.
- 38 Bryce, T. A., Welti, D., Walsby, A. E. and Nichols, B. W.: Monohexoside derivatives of long-
39 chain polyhydroxy alcohols; a novel class of glycolipid specific to heterocystous algae,
40 *Phytochem.*, 11, 295–302, doi:10.1016/S0031-9422(00)90006-2, 1972.

- 1 Capone, D. G., Burns, J. A., Montoya, J. P., Subramaniam, A., Mahaffey, C., Gunderson, T.,
2 Michaels, A. F. and Carpenter, E. J.: Nitrogen fixation by *Trichodesmium* spp.: An important
3 source of new nitrogen to the tropical and subtropical North Atlantic Ocean, Global
4 Biogeochem. Cycles, 19(2), GB2024, doi:10.1029/2004GB002331, 2005.
- 5 Celepli, N., Sundh, J., Ekman, M., Dupont, C. L., Yoosseph, S., Bergman, B., and Ininbergs,
6 K.: Meta-omic analyses of Baltic Sea cyanobacteria: Diversity, community structure and salt
7 acclimation. Environm. Microbiol., 19, 673–686, doi:10.1111/1462-2920.13592, 2017.
- 8 Emeis, K.-C., Neumann, T., Endler, R., Struck, U., Kunzendorf, H. and Christiansen, C.:
9 Geochemical records of sediments in the Eastern Gotland Basin—products of sediment
10 dynamics in a not-so-stagnant anoxic basin?, App. Geochem., 13(3), 349–358,
11 doi:10.1016/S0883-2927(97)00104-2, 1998.
- 12 Emerson, S. and Hedges, J.: Chemical oceanography and the marine carbon cycle, Cambridge
13 University Press., 2008.
- 14 Finni, T., Kononen, K., Olsonen, R. and Wallström, K.: The History of Cyanobacterial
15 Blooms in the Baltic Sea, Ambio, 30(4), 172–178, doi:10.1579/0044-7447-30.4.172, 2001.
- 16 Fritz, S. C.: Lake Development and Limnological Response to Prehistoric and Historic Land-
17 Use in Diss, Norfolk, U.K., J. Ecol., 77(1), 182–202, doi:10.2307/2260924, 1989.
- 18 Funkey, C. P., Conley, D. J., Reuss, N. S., Humborg, C., Jilbert, T. and Slomp, C. P.: Hypoxia
19 Sustains Cyanobacteria Blooms in the Baltic Sea, Environ. Sci. Technol., 48(5), 2598–2602,
20 doi:10.1021/es404395a, 2014.
- 21 Gambacorta, A., Soriente, A., Trincone, A. and Sodano, G.: Biosynthesis of the heterocyst
22 glycolipids in the cyanobacterium *Anabaena cylindrica*., Phytochem., 39(4), 771–774,
23 doi:10.1016/0031-9422(95)00007-T, 1995.
- 24 Gambacorta, A., Pagnotta, E., Romano, I., Sodano, G. and Trincone, A.: Heterocyst
25 glycolipids from nitrogen-fixing cyanobacteria other than *Nostocaceae*., Phtytochem., 48(5),
26 801–205, 1998.
- 27 Gustafsson, B. G. and Westman, P.: On the causes for salinity variations in the Baltic Sea
28 during the last 8500 years, Paleoceanography, 17, 1040–1, doi:10.1029/2000PA000572, 2002.
- 29 Hajdu, S., Höglander, H. and Larsson, U.: Phytoplankton vertical distributions and
30 composition in Baltic Sea cyanobacterial blooms, Harmful Algae, 6(2), 189–205,
31 doi:10.1016/j.hal.2006.07.006, 2007.
- 32 Hällfors, G.: Checklist of Baltic Sea Phytoplankton Species (including some heterotrophic
33 protistan groups), Baltic Sea Environment Proceedings, 95, 1–208, 2004.
- 34 Hansson, M. and Öberg, J.: Cyanobacterial blooms in the Baltic Sea in 2010, HELCOM
35 Baltic Sea Environ. Fact Sheets [online] Available from: <http://www.helcom.fi/baltic-sea-trends/environment-fact-sheets/eutrophication/cyanobacterial-blooms-in-the-baltic-sea>, n.d.
- 37 Hyvarinen, H.: The Mastogloia Stage in Baltic Sea History: Diatom Evidence from Southern
38 Finland, B. Geo. Soc. Finland, 56(1–2), 99–116, 1984.

- 1 Jensen, J. B., Bennike, O., Witkowski, A., Lemke, W. and Kuijpers, A.: Early Holocene
2 history of the southwestern Baltic Sea: The Ancylus Lake stage, *Boreas*, 28(4), 437–453,
3 doi:10.1111/j.1502-3885.1999.tb00233.x, 1999.
- 4 Kabel, K., Moros, M., Porsche, C., Neumann, T., Adolphi, F., Andersen, T. J., Siegel, H.,
5 Gerth, M., Leipe, T., Jansen, E., Damsté, S. and S. J.: Impact of climate change on the Baltic
6 Sea ecosystem over the past 1,000 years, *Nat. Clim. Change*, 2(12), 871–874,
7 doi:<http://dx.doi.org/10.1038/nclimate1595>, 2012.
- 8 Kahru, M.: Monitoring algal blooms : new techniques for detecting large-scale environmental
9 change, Springer, Berlin ; New York., 1997.
- 10 Kahru, M. and Elmgren, R.: Multidecadal time series of satellite-detected accumulations of
11 cyanobacteria in the Baltic Sea, *Biogeosciences*, 11, 3619–3633, doi:10.5194/bg-11-3619-
12 2014, 2014.
- 13 Kahru, M., Horstmann, U. and Rud, O.: Satellite detection of increased cyanobacteria blooms
14 in the Baltic Sea: Natural fluctuation or ecosystem change?, *Ambio. Stockholm*, 23, 469–472,
15 1994.
- 16 Kahru, M., Savchuk, O. P. and Elmgren, R.: Satellite measurements of cyanobacterial bloom
17 frequency in the Baltic Sea: interannual and spatial variability, *Mar. Ecol.-Prog. Ser.*, 343,
18 15–23, doi:10.3354/meps06943, 2007.
- 19 Kanoshina, I., Lips, U. and Leppänen, J.-M.: The influence of weather conditions
20 (temperature and wind) on cyanobacterial bloom development in the Gulf of Finland (Baltic
21 Sea), *Harmful Algae*, 2(1), 29–41, doi:10.1016/S1568-9883(02)00085-9, 2003.
- 22 Karjalainen, M., Engström-Ost, J., Korpinen, S., Peltonen, H., Pääkkönen, J.-P., Rönkkönen,
23 S., Suikkanen, S. and Viitasalo, M.: Ecosystem consequences of cyanobacteria in the northern
24 Baltic Sea, *Ambio*, 36(2–3), 195–202, 2007.
- 25 Karl, D., Letelier, R., Tupas, L., Dore, J., Christian, J. and Hebel, D.: The role of nitrogen
26 fixation in biogeochemical cycling in the subtropical North Pacific Ocean, *Nature*, 388(6642),
27 533–538, doi:10.1038/41474, 1997.
- 28 Kononen, K.: Dynamics of the toxic cyanobacterial blooms in the Baltic Sea, University of
29 Helsinki., 1992.
- 30 Kononen, K., Kuparinen, J., Kalervo, M., Laanemets, J., Pavelson, J. and Nömmann, S.:
31 Initiation of cyanobacterial blooms in a frontal region at the entrance to the Gulf of Finland,
32 Baltic Sea., *Limnol. Oceanogr.*, 41(1), 98–112, doi:10.4319/lo.1996.41.1.0098, 1996.
- 33 Kutser, T., Metsamaa, L., Strömbeck, N. and Vahtmäe, E.: Monitoring cyanobacterial blooms
34 by satellite remote sensing, *Estuarine, Coastal and Shelf Science*, 67(1), 303–312,
35 doi:10.1016/j.ecss.2005.11.024, 2006.
- 36 Lambein, F. and Wolk, C. P.: Structural studies on the glycolipids from the envelope of the
37 heterocyst of *Anabaena cylindrica.*, *Biochemistry*, 12(5), 791–798, 1973.

- 1 Mazur-Marzec, H., Żeglińska, L. and Pliński, M.: The effect of salinity on the growth, toxin
2 production, and morphology of *Nodularia spumigena* isolated from the Gulf of Gdańsk,
3 southern Baltic Sea, *J. Appl. Phycol.*, 17(2), 171–179, doi:10.1007/s10811-005-5767-1, 2005.
- 4 McGowan, S., Britton, G., Haworth, E. and Moss, B.: Ancient blue-green blooms, *Limnol.*
5 *Oceanogr.*, 44(2), 436–439, doi:10.4319/lo.1999.44.2.0436, 1999.
- 6 Moisander, P. H., McClinton, E. and Paerl, H. W.: Salinity effects on growth, photosynthetic
7 parameters, and nitrogenase activity in estuarine planktonic cyanobacteria, *Microb. Ecol.*,
8 43(4), 432–442, doi:10.1007/s00248-001-1044-2, 2002.
- 9 Moore, E. K., Hopmans, E. C., Rijpstra, W. I. C., Villanueva, L., Dedysh, S. N.,
10 Kulichevskaya, I. S., Wienk, H., Schouten, F. and Sinninghe Damsté, J. S.: Novel mono-, di-,
11 , and trimethylornithine membrane lipids in northern wetland Planctomycetes, *Appl. Environ.*
12 *Microbiol.*, 79(22), 6874–6884, doi:10.1128/AEM.02169-13, 2013.
- 13 Murry, M. A. and Wolk, C. P.: Evidence that the barrier to the penetration of oxygen into
14 heterocysts depends upon two layers of the cell envelope, *Archives of Microbiology*, 151,
15 469–474, doi:10.1007/BF00454860, 1989.
- 16 Nichols, B. W. and Wood, B. J. B.: New Glycolipid specific to Nitrogen-fixing Blue-green
17 Algae., *Nature*, 217, 767–768, doi:10.1038/217767a0, 1968.
- 18 Paerl, H.: Nutrient and other environmental controls of harmful cyanobacterial blooms along
19 the freshwater–marine continuum, SpringerLink, 217–237, doi:10.1007/978-0-387-75865-
20 7_10, 2008.
- 21 Paerl, H. W.: Nuisance phytoplankton blooms in coastal, estuarine, and inland waters1,
22 *Limnol. Oceanogr.*, 33(4part2), 823–843, doi:10.4319/lo.1988.33.4part2.0823, 1988.
- 23 Paerl, H. W. and Huisman, J.: Climate change: a catalyst for global expansion of harmful
24 cyanobacterial blooms, *Environ. Microbiol. Rep.*, 1(1), 27–37, doi:10.1111/j.1758-
25 2229.2008.00004.x, 2009.
- 26 Paerl, H. W., Hall, N. S. and Calandrino, E. S.: Controlling harmful cyanobacterial blooms in
27 a world experiencing anthropogenic and climatic-induced change, *Sci. Total Environ.*,
28 409(10), 1739–1745, doi:10.1016/j.scitotenv.2011.02.001, 2011.
- 29 Pitarch, J., Volpe, G., Colella, S., Krasemann, H. and Santoleri, R.: Remote sensing of
30 chlorophyll in the Baltic Sea at basin scale from 1997 to 2012 using merged multi-sensor
31 data, *Ocean Sci.*, 12(2), 379–389, doi:10.5194/os-12-379-2016, 2016.
- 32 Ploug, H.: Cyanobacterial surface blooms formed by *Aphanizomenon* sp. and *Nodularia*
33 *spumigena* in the Baltic Sea: Small-scale fluxes, pH, and oxygen microenvironments.,
34 *Limnol. Oceanogr.*, 53(3), 914–921, doi:10.4319/lo.2008.53.3.0914, 2008.
- 35 Poutanen, E. L. and Nikkilä, K.: Carotenoid pigments as tracers of cyanobacterial blooms in
36 recent and postglacial sediments of the Baltic Sea, *Ambio*, 30(4–5), 179–183, 2001.
- 37 Rejmánková, E., Komárková, J. and Rejmánek, M.: $\delta^{15}\text{N}$ as an indicator of N_2 -fixation by
38 cyanobacterial mats in tropical marshes, *Biogeochemistry*, 67(3), 353–368,
39 doi:10.1023/B:BIOG.0000015790.28584.ed, 2004.

- 1 Rippka, R., Deruelles, J., Waterbury, J. B., Herdman, M. and Stanier, R. Y.: Generic
2 Assignments, Strain Histories and Properties of Pure Cultures of Cyanobacteria,
3 Microbiology, 111(1), 1–61, doi:10.1099/00221287-111-1-1, 1979.
- 4 Schouten, S., Villareal, T. A., Hopmans, E. C., Mets, A., Swanson, K. M. and Sinninghe
5 Damsté, J. S.: Endosymbiotic heterocystous cyanobacteria synthesize different heterocyst
6 glycolipids than free-living heterocystous cyanobacteria., Phytochem., 85, 115–21,
7 doi:10.1016/j.phytochem.2012.09.002, 2013.
- 8 Schweger, C. E. and Hickman, M.: Holocene paleohydrology of central Alberta: testing the
9 general-circulation-model climate simulations, Can. J. Earth Sci., 26, 1826–1833,
10 doi:10.1139/e89-155, 1989.
- 11 Sinninghe Damsté, J. S., Rijpstra, W. I. C. and Reichart, G.: The influence of oxic degradation
12 on the sedimentary biomarker record II. Evidence from Arabian Sea sediments, Geochim.
13 Cosmochim. Acta, 66(15), 2737–2754, doi:10.1016/S0016-7037(02)00865-7, 2002.
- 14 Sivonen, K., Halinen, K., Sihvonen, L. M., Koskenniemi, K., Sinkko, H., Rantasärkkä, K.,
15 Moisander, P. H. and Lyra, C.: Bacterial diversity and function in the Baltic Sea with an
16 emphasis on cyanobacteria., Ambio, 36(2), 180–185, doi:10.1579/0044-
17 7447(2007)36[180:bdafit]2.0.co;2, 2007.
- 18 Soriente, A., Gambacorta, A., Trincone, A., Sili, C., Vincenzini, M. and Sodano, G.:
19 Heterocyst glycolipids of the cyanobacterium *Cyanospira rippkae*, Phytochem., 33(2), 393–
20 396, 1993.
- 21 Staal, M., Meysman, F. J. R. and Stal, L. J.: Temperature excludes N₂ fixing heterocystous
22 cyanobacteria in the tropical oceans, Nature, 425(6957), 504–507, doi:10.1038/nature01999,
23 2003.
- 24 Stal, L. J.: Is the distribution of nitrogen-fixing cyanobacteria in the oceans related to
25 temperature?, Environ. Microbiol., 11(7), 1632–1645, doi:10.1111/j.1758-
26 2229.2009.00016.x, 2009.
- 27 Stipa, T.: The dynamics of the N/P ratio and stratification in a large nitrogen-limited estuary
28 as a result of upwelling: a tendency for offshore *Nodularia* blooms, Hydrobiologia, 487(1),
29 219–227, doi:10.1023/A:1022990116669, 2002.
- 30 Sun, M.-Y. and Wakeham, S. G.: Molecular evidence for degradation and preservation of
31 organic matter in the anoxic Black Sea Basin, Geochim. Cosmochim. Acta, 58(16), 3395–
32 3406, doi:10.1016/0016-7037(94)90094-9, 1994.
- 33 Walsby, A. E.: The permeability of heterocysts to the gases nitrogen and oxygen., Proc. Royal
34 Soc. London, 226(1244), 345–366, doi:10.1098/rspb.1985.0099, 1985.
- 35 Warden, L. A.: Paleoenvironmental reconstructions in the Baltic Sea and Iberian Margin, PhD
36 thesis University of Utrecht, 2017.
- 37 Warden, L. Moros, M., Neumann, T., Shennan, S., Timpson, A., Manning, K., Sollai, M.,
38 Wacker, L., Perner, K., Häusler, K., Leipe, T., Zillén, L., Kotilainen, A., Jansen, E.,
39 Schneider, R. R., Oeberst, R., Arz, H., and Sinninghe Damsté, J.S.: Climate induced human

- 1 demographic and cultural change in northern Europe during the mid-Holocene. *Sci. Rep.*, 7,
2 15251, doi:10.1038/s41598-017-14353-5, 2017.
- 3 Wasmund, N.: Occurrence of cyanobacterial blooms in the Baltic Sea in relation to
4 environmental conditions, *Int. Revue ges. Hydrobiol. Hydrogr.*, 82(2), 169–184,
5 doi:10.1002/iroh.19970820205, 1997.
- 6 Wasmund, N. and Uhlig, S.: Phytoplankton trends in the Baltic Sea, *ICES J. Mar. Sci.*, 60(2),
7 177–186, doi:10.1016/S1054-3139(02)00280-1, 2003.
- 8 Whitton, B. A. and Potts, M.: Introduction to Cyanobacteria, in *Ecology of Cyanobacteria II. Their Diversity in Space and Time*, edited by B. A. Whitton, pp. 1–15, Springer., 2012.
- 10 Wolk, C. P.: Heterocysts, in: *The Biology of Cyanobacteria*, edited by Carr, N. G. and
11 Whitton, B. A., pp. 359–386, Blackwell Scientific Publishers, Oxford, 1982.
- 12 Wörmer, L., Cires, S., Velazquez, D., Quesada, A. and Hinrichs, K.-U.: Cyanobacterial
13 heterocyst glycolipids in cultures and environmental samples: Diversity and biomarker
14 potential, *Limnol. Oceanogr.*, 57(6), 1775–1788, doi:10.4319/lo.2012.57.06.1775, 2012.
- 15 Zakrisson, A., Larsson, U. and Höglander, H.: Do Baltic Sea diazotrophic cyanobacteria take
16 up combined nitrogen in situ?, *J. Plankton Res.*, 36(5), 1368–1380,
17 doi:10.1093/plankt/fbu053, 2014.
- 18 Zillén, L. and Conley, D. J.: Hypoxia and cyanobacteria blooms - are they really natural
19 features of the late Holocene history of the Baltic Sea?, *Biogeosciences*, 7(8), 2567–2580,
20 doi:10.5194/bg-7-2567-2010, 2010.
- 21 Züllig, H.: Carotenoids from plankton and photosynthetic bacteria in sediments as indicators
22 of trophic changes in Lake Lobsigen during the last 14000 years, *Hydrobiologia*, 143(1), 315–
23 319, doi:10.1007/BF00026676, 1986.

24

25
26
27

Table 1. Distribution of the six targeted HGs in sediments from this study and from cultures of selected heterocystous cyanobacteria. Key: (++) Dominant (>25%); (+) Minor presence (5-25%); (tr.) Traces (<5%); (-) Not detected or not reported. Underlined strains were isolated from the Baltic Sea.

Baltic Sediment		C ₂₆ diol	C ₂₆ keto-ol	C ₂₈ diol	C ₂₈ keto-ol	C ₂₈ triol	C ₂₈ keto-diol
MoWP		++	+	tr.	tr.	+	+
Pre-MoWP brackish		++	+/tr.	+	tr.	+/tr.	tr.
Ancylus Lake-II		++	+/tr	++/+	tr/-	tr/-	-
Ancylus Lake-I		++	++/+	++/-	++/tr	+/tr	+/tr
Yoldia Sea		++	+	++/+	+/tr	+/tr	tr
Nostocaceae cultures	Strain ID						
<u><i>Nodularia</i> sp.^a</u>	<u>CCY 9414 & 9416</u>	++	+	-	-	-	-
<u><i>Nodularia</i> sp.^b</u>	<u>BY1</u>	++	+	-	-	-	-
<u><i>Nodularia</i> sp.^b</u>	<u>F81</u>	++	+	-	-	-	-
<u><i>Nodularia</i> sp.^b</u>	<u>AV1</u>	++	+	-	-	-	-
<u><i>Nodularia</i> sp.^b</u>	<u>HEM</u>	++	+	-	-	-	-
<i>Nodularia chucula</i> ^a	CCY 0103	++	+	-	-	-	-
<i>Aphanizomenon</i> sp. ^a	CCY 0368	++	+	+	-	-	-
<u><i>Aphanizomenon</i> sp.^a</u>	<u>CCY 9905</u>	++	+	+	+	tr.	tr.
<u><i>Aphanizomenon</i> sp.^b</u>	<u>TR183</u>	++	+	tr.	-	+	tr.
<i>A. aphanizomenoides</i> ^c	UAM 523	+	-	++	+	tr	-
<i>A. gracile</i> ^c	UAM 521	++	++	tr.	-	tr.	-
<i>A. ovalisporum</i> ^{c,f}	UAM 290	++	tr.	tr.	tr.	-	-
<i>Anabaena</i> sp. ^a	CCY 0017, 9910,	++	+	+	+	-	-
<i>Anabaena</i> sp. ^a	CCY 9402	-	-	++	+	-	-
<i>Anabaena</i> sp. ^a	CCY 9613	+	+	-	-	-	-
<i>Anabaena</i> sp. ^a	CCY 9614, 9922	++	+	-	-	-	-
<u><i>Anabaena</i> sp.^b</u>	<u>315</u>	++	++	tr.	tr.	tr.	-
<u><i>Anabaena</i> sp.^b</u>	<u>BIR53</u>	++	++	tr.	tr.	tr.	-
<u><i>Anabaena</i> sp.^b</u>	<u>BIR169</u>	++	+	tr.	tr.	++	+
<i>Anabaena cylindrica</i> ^a	CCY 9921	++	+	-	-	-	-
<i>Anabaenopsis</i> sp. ^a	CCY 0520	++	+	+	-	-	-
<i>Nostoc</i> sp. ^a	CCY 0012, 9926	++	+	-	-	-	-
<i>Nostoc</i> sp. ^c	MA 4	++	++	tr.	-	tr.	-
<i>Cylindrospermopsis raciborskii</i> ^{c,f}	UAM 520	++	tr.	+	tr.	+	-
<i>Cyanospira rippkae</i> ^e	ATCC 43194	-	-	++	+	-	-
Rivulariaceae cultures							
<i>Calothrix desertica</i> ^d	PCC 7102	-	-	-	-	++	++
<i>Calothrix</i> sp. ^c	MU 27	-	-	tr.	-	++	++
<i>Calothrix</i> sp. ^a	CCY 0018	-	-	-	-	++	+
<i>Calothrix</i> sp. ^a	CCY 0202	tr.	tr.	-	-	++	+
<i>Calothrix</i> sp. ^a	CCY 0327	-	-	-	-	++	+
<i>Calothrix</i> sp. ^a	CCY 9923	-	-	+	+	++	+
Microchaetaceae cultures							
<i>Microchaete</i> sp. ^{d,f}	PCC 7126	-	-	+	++	-	-
Tolypothrichaceae cultures							
<i>Tolypothrix tenuis</i> ^{d,f}	PCC 7101	-	-	++	+	-	-

a = Bauersachs et al. (2009a), b = Bauersachs et al. (2017), c = Wörmer et al. (2012), d = Gambacorta et al. (1998), e = Soriente et al. (1993), f = these species also contain HGs other than the six HGs targeted in this study

28 **Table 2.** Analysis of HGs in Baltic sediments by Orbitrap MS. Key: (++) Dominant (>25%); (+) Minor presence (5-25%); (tr.) Traces (<5%); (-)
 29 Not detected. Relative abundances are based on peak areas.

Sample	C5 26 diol	Deoxy C6 26 diol	C6 26 diol ^a	C6 26 keto-ol	C6 28 diol	C6 28 keto-ol	C6 28 triol	C6 28 keto- diol	C6 30 triol	C6 30 keto- diol	C6 32 triol	C6 32 keto- diol
P435-1-4 MUC 4	-	-	++	+	tr.	tr.	++	+	-	-	-	-
P435-1-4 MUC 35	-	-	++	+	tr.	-	+	+	-	-	-	-
P435-1-4 MUC 62	-	-	++	+	tr.	-	++	+	-	-	-	-
P435-1-4 MUC 99	-	-	++	tr.	tr.	-	++	tr	-	-	-	-
GC 1-2 cm	-	-	++	tr.	tr.	-	+	-	-	-	-	-
GC 5-6 cm	-	-	++	tr.	tr.	-	+	-	-	-	-	-
GC 17-18 cm	-	-	++	tr.	tr.	-	+	-	-	-	-	-

^asum of two isomers

31 **Figure legends**

32

33 **Figure 1.** Structures of the C₆ heterocyst glycolipids (HG) targeted by the study. C₂₆ diol HG
34 (1-(O-hexose)-3,25-hexacosanediol); C₂₆ keto-ol HG (1-(O-hexose)-3-keto-25-hexacosanol);
35 C₂₈ diol HG (1-(O-hexose)-3,27-octacosanediol); C₂₈ keto-ol HG (1-(O-hexose)-3-keto-27-
36 octacosanol); C₂₈ triol HG (1-(O-hexose)-3,25,27-octacosanetriol); C₂₈ keto-diol HG (1-(O-
37 hexose)-27-keto-3,25-octacosanediol).

38

39 **Figure 2.** Map of the Baltic Sea. The location of multicore (MUC) P435-1-4 and gravity core
40 (GC) 303600 in the eastern Gotland Basin is indicated with a black star (modified from
41 Warden et al., 2017).

42

43 **Figure 3.** Proxy records of the Baltic Sea cores on a composite depth scale aligned with core
44 photos showing the lamination of the sediments of the post-Ancylus Lake stage. **(a)** The
45 abundance of the HGs (r.u. gTOC⁻¹) on a log scale, **(b)** δ¹⁵N (‰), **(c)** TOC content (%) partly
46 derived from Warden et al. (2017), and **(d)** TEX₈₆-derived summer sea surface temperatures
47 (SSTs) from Kabel et al. (2012) and Warden et al. (2017). Data points derived from the MUC
48 P435-1-4 core are in grey and those from the GC 303600 core are in black. The stratigraphy is
49 based on age models published elsewhere (Kabel et al., 2012; Warden et al., 2017) and for the
50 deeper part of the GC 303600 core on unpublished data on diatom assemblages. The TEX₈₆
51 data of Kabel et al. (2012) were measured on a different core (MUC 303600) obtained from
52 the same site, which was correlated to the MUC P435-1-4 core based on the TOC profiles
53 (Fig. S1). Note that phases characterized by deposition of laminated sediments are the periods
54 during the Holocene when the bottom waters of the Baltic Sea were anoxic.

55

56 **Figure 4.** Distribution of HGs, displayed as fractional abundance (%), versus depth (in cm)
57 for **(a)** the MUC P435-1-4 core, and **(b)** the GC 303600 core. Colour key: light green: C₂₈
58 triol HG; blue: C₂₈ keto-diol HG; yellow: C₂₈ diol HG; orange: C₂₈ keto-ol HG; purple: C₂₆
59 diol HG; red: C₂₆ keto-ol HG. Each sample represents a sediment slice of 0.5 cm in the case
60 of the MUC and of 1 or 2 cm in the case of the GC. The stratigraphy of the cores (see Fig. 3)
61 is indicated. The scores on PC1 and PC2 derived from the principal component analysis of the
62 HG distribution are plotted along the fractional abundance plots using the same scale for both
63 cores.

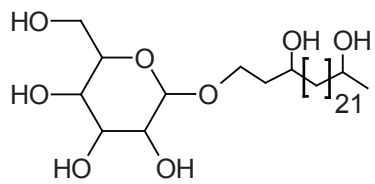
64

65 **Figure 5.** Principal component analysis of the heterocyst glycolipids (HGs) distribution in the
66 sediments recovered by the MUC P435-1-4 and the GC 303600 cores from the Gotland Basin,
67 Baltic Sea. **(a)** The loadings of the six HGs on the first two PCs, with PC1 accounting for the
68 47% and PC2 for 29% of the variance. **(b)** Scores of the sediments from various stages on
69 PC1 and PC2.

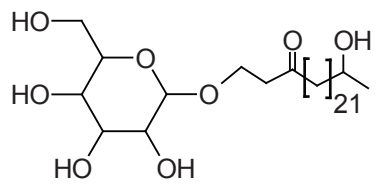
70

71 **Figure 6.** Abundance of heterocyst glycolipids (HG) in the Baltic Sea over the period 1977–
72 2012 (from MUC) compared with the fractional cyanobacteria accumulation (FCA, %) from
73 the time period 1979–2012, as reported by Kahru et al. (2014).

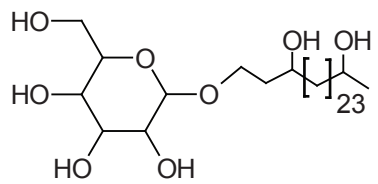
Figure 1



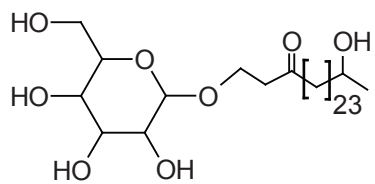
C₂₆ diol



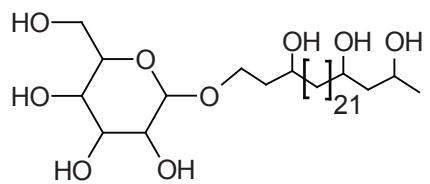
C₂₆ keto-ol



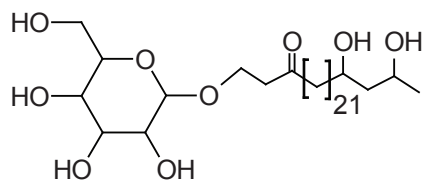
C₂₈ diol



C₂₈ keto-ol



C₂₈ triol



C₂₈ keto-diol

Figure 2

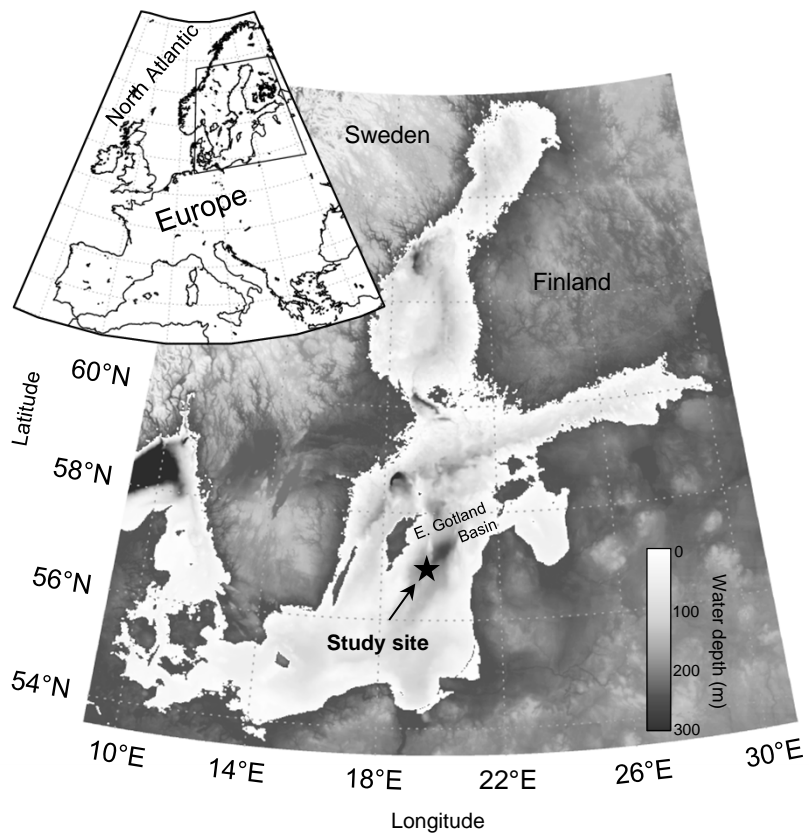


Figure 3

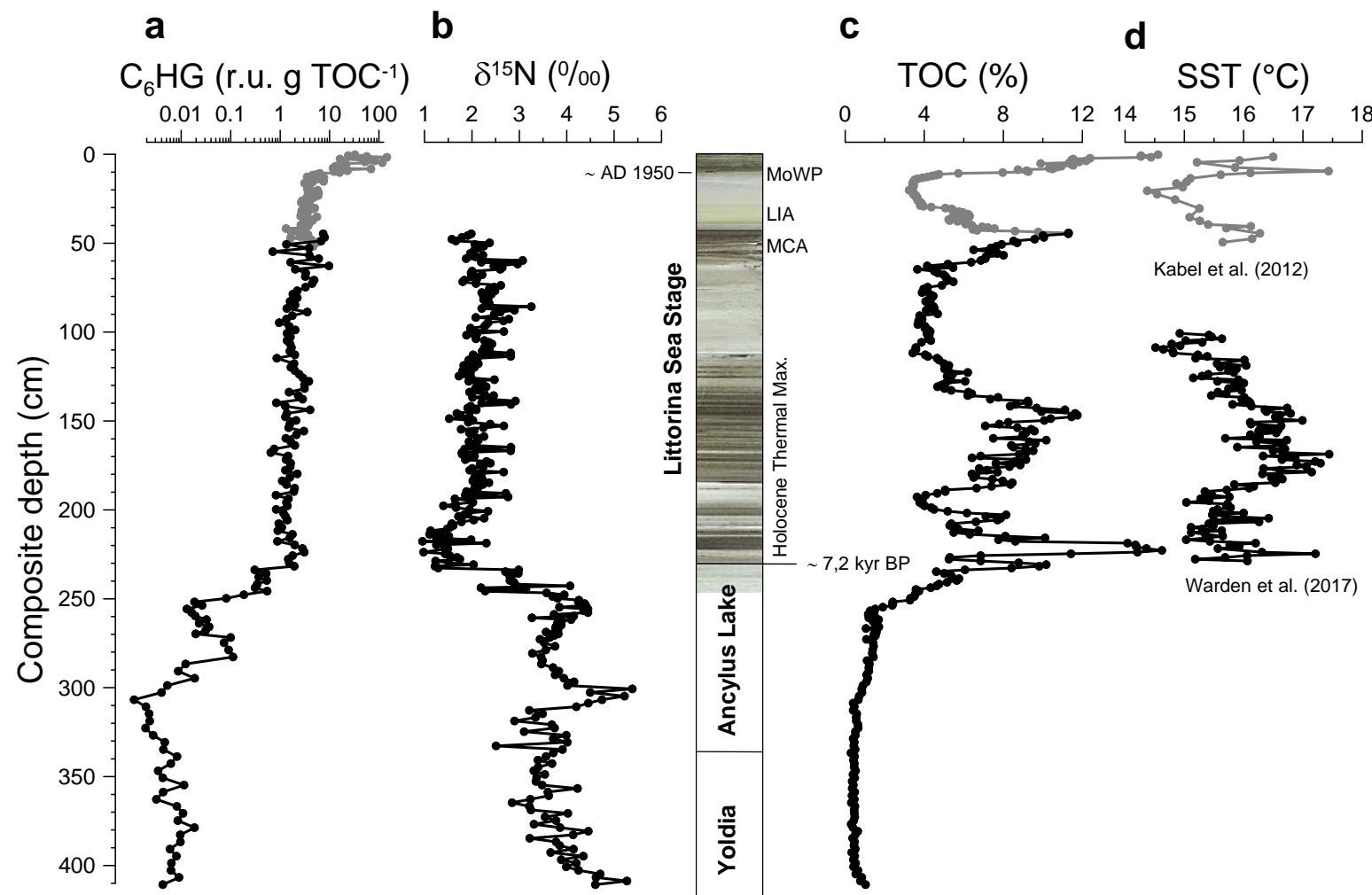
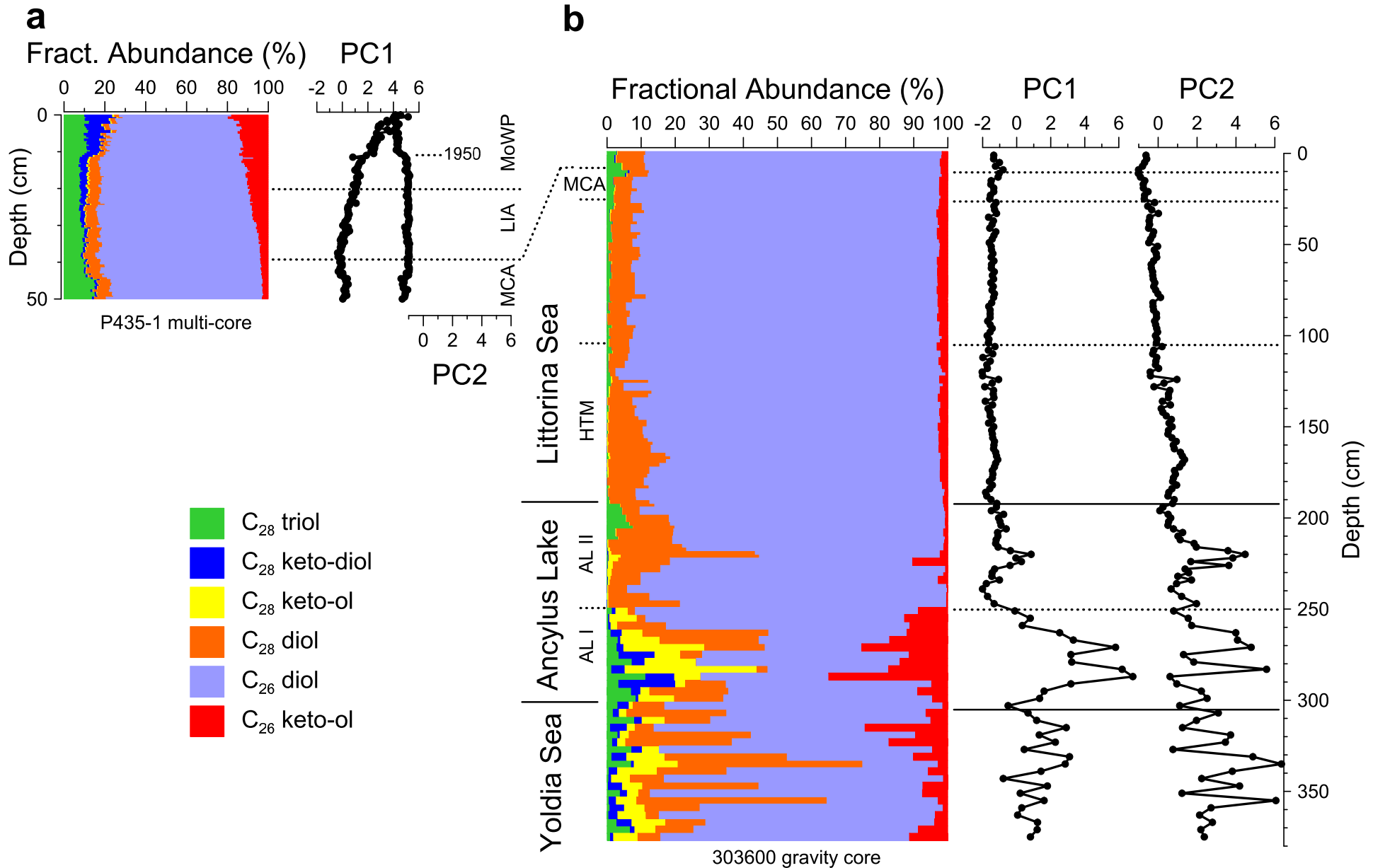


Figure 4



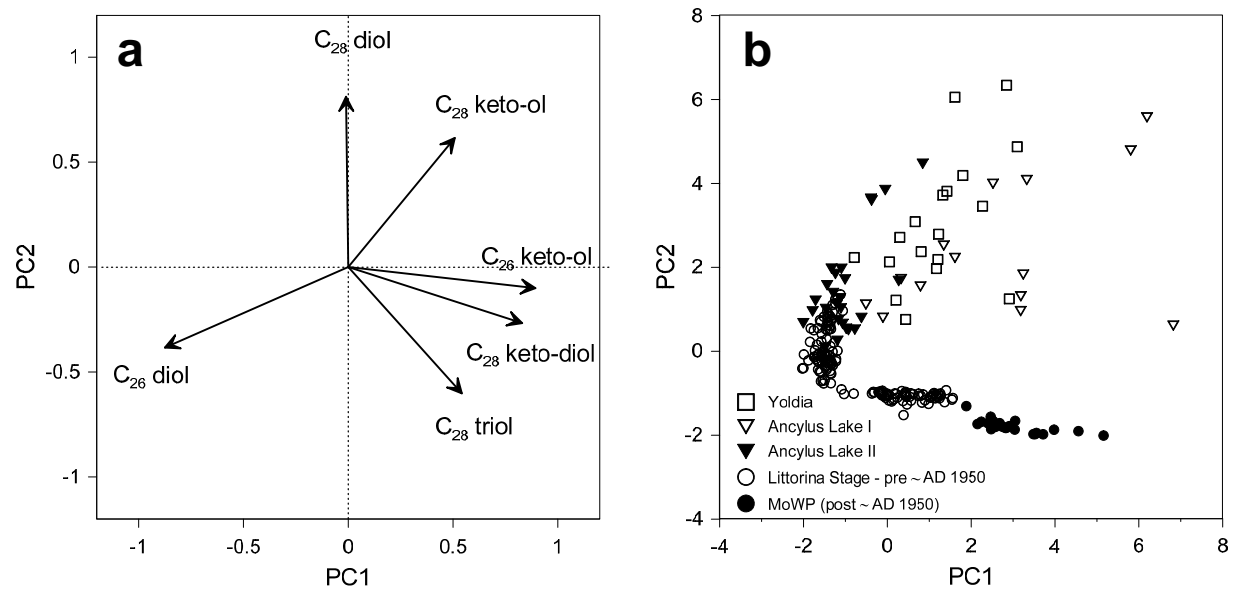
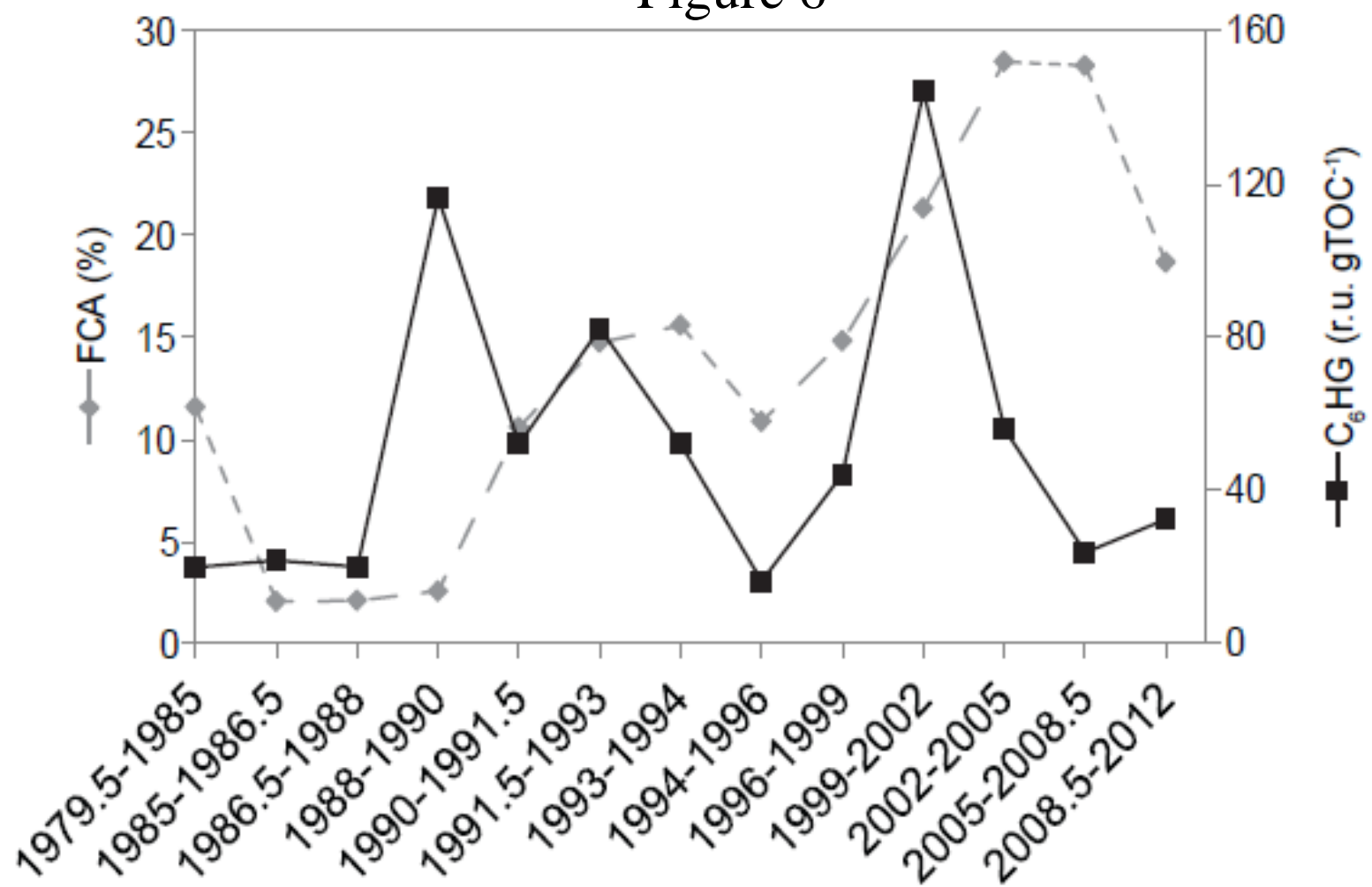


Figure 5

Figure 6



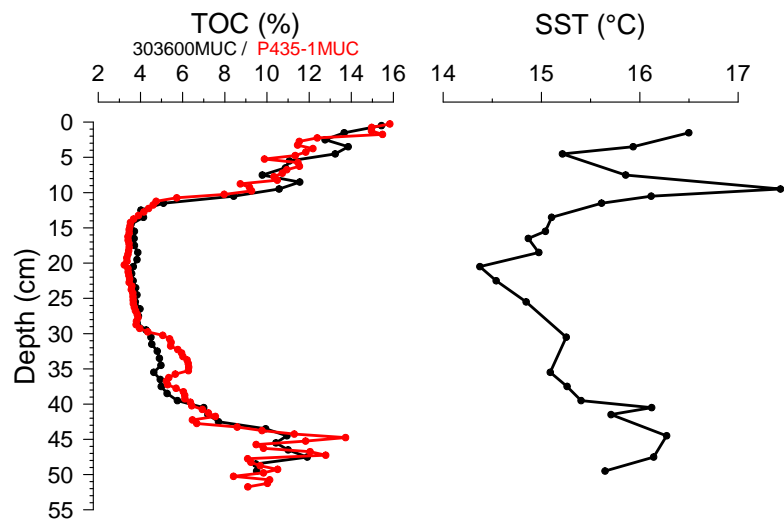


Figure S1: Correlation of the MUC cores 303600 (Kabel et al., 2012) and P435-1 (this work) on the basis of the TOC content. SST data is from MUC 303600 (Kabel et al., 2012).